Notes on charmed baryons

Gert Aarts, April 14, 2020

1 Nomenclature

Taken from Wikipedia [1]. The nomenclature of charmed baryons is based on both quark content and isospin. The naming follows the rules established by the Particle Data Group.

- cud: isospin 0, charmed Λ's: Λ_c.
- cuu, cud, cdd: isospin 1, charmed Σ's: Σ_c.
- cus, cds: charmed Ξ's: Ξ_c and Ξ_c', isospin 1/2.
- css: charmed Ω's: Ω_c, isospin 0.
- ccu, ccd: double charmed Ξ's: Ξ_{cc}, isospin 1/2.
- ccs: double charmed Ω's: Ω_{cc}, isospin 0.
- ccc: triple charmed Ω's: Ω_{ccc}, isospin 0.

2 SU(4) multiplet

Taken from Refs. [2, 3]. Baryons made from u, d, s, and c quarks belong to SU(4) multiplets, see Fig. 1. The baryons in a given multiplet all have the same spin and parity.

More details for $C \neq 0$ are given in Refs. [2, 4, 5], including the masses and other properties. Quark content:

$$
\begin{array}{lllll}
 & & \Lambda_c^+ = udc, & & \\
C = 1: & \Sigma_c^{++} = uuc, & \Sigma_c^+ = udc, & \Sigma_c^0 = ddc, & \\
 & & \Xi_c^+ = usc, & \Xi_c^0 = dsc, & \\
 & & \Xi_c^{\prime +} = usc, & \Xi_c^{\prime 0} = dsc, & \\
 & & & \Omega_c^0 = ssc, & \\
C = 2: & \Xi_{cc}^{++} = ucc, & \Xi_{cc}^+ = dcc, & & \\
 & & \Omega_{cc}^+ = scc, & & \\
C = 3: & \Omega_{ccc}^{++} = ccc. & & &
\end{array}
$$

A useful lattice paper on charmed baryons is Ref. [8].

3 Data

All ensembles have at least 1000 configs with 8 sources, so at least 8000 measurements. The results in vacuum are from $N_\tau = 128$ for Gen2L.

From Ben's email:

— There are three new 'Lambda' type Baryons, i.e. uds, udc and usc (filenames lambda.3fl). There are three new 'Sigma' type Baryons with spin 1/2, i.e. uds, udc and usc (filename sigma12.3fl) There are three new 'Sigma*' type Baryons with spin 3/2, i.e. uds, udc and usc (filename sigma32.3fl)

Please note that the name reflects the contraction operators (i.e. Lattice operator in Gattringer etc), so in the PDG or Wikipedia typically they are either Sigmas or Xis. Some particles are already there, so these should be consistent. —

4 Ξ_{cc}

For interest in Ξ_{cc}^{++} from the perspective of heavy-ion collisions, see Ref. [6].

5 R parameter

In Fig. 4 we show the baryon R parameter in all channels. The R parameter is distinctly nonzero and close to 1 in vacuum and is reduced in the high-temperature phase. For massless quark, we expect $R = 0$ in the chirally unbroken phase (absence of parity doubling). With massive quarks, chiral symmetry is explicitly broken and we expect $R \to 0$ as $m_q/T \to 0$. This is clearly visible in Fig. 4, where at the highest temperature the R values are ordered based on the (heavy) quark content.

The transition between the low- and the high-temperature phase can be identified by the inflection point in the R curve. There is an inflection point in all channels, except the doubly charmed $J = \frac{1}{2}$ channels (Ξ_{cc}, Ω_{cc}) and the $J = \frac{3}{2}$ Ω_{ccc} channel. The inflection point temperatures are given in table 4. We notice a remarkable consistency between these temperatures, with only a slightly higher value for charmed Ω channels.

6 Effective masses for baryons

With one pole for the positive- and negative-parity states each, the correlator takes the form

$$G(\tau) = Ae^{-m_+\tau} + Be^{-m_-(1/T-\tau)}. \tag{1}$$

Spin	Particle	Ben's name.dat 11/19	Ben's name 03/20
$\frac{1}{2}$	N	doublet.2fl.uud	id (1)
	Σ	doublet.2fl.uus	id (1), **sigma12.3fl.uds (0)**
	Λ	not computed	**lambda.3fl.uds (0)**
	Ξ	doublet.2fl.ssu	id (0)
	Λ_c	not computed	**lambda.3fl.udc (1)**
	Σ_c	doublet.2fl.uuc	id (2), **sigma12.3fl.udc (1)**
	Ξ_c	not computed	**lambda.3fl.usc (1)**
	Ξ'_c	not computed	**sigma12.3fl.usc (1)**
	Ξ_{cc}	doublet.2fl.ccu	id (2)
	Ω_c	doublet.2fl.ssc	id (0)
	Ω_{cc}	doublet.2fl.ccs	id (1)
$\frac{3}{2}$	Δ	quadruplet.1fl.uuu, .2fl.uud	id (2), (1)
	Σ^*	quadruplet.2fl.uus	id (1), **sigma32.3fl.uds (0)**
	Ξ^*	quadruplet.2fl.ssu	id (0)
	Ω	quadruplet.1fl.sss	id (-1)
	Σ_c	quadruplet.2fl.uuc	id (2), **sigma32.3fl.udc (1)**
	Ξ_c	not computed	**sigma32.3fl.usc (1)**
	Ω_c	quadruplet.2fl.ssc	id (0)
	Ξ_{cc}	quadruplet.2fl.ccu	id (2)
	Ω_{cc}	quadruplet.2fl.ccs	id (1)
	Ω_{ccc}	quadruplet.1fl.ccc	id (2)

Table 1: Ben's naming scheme for Gen2L. 'id' means 'identical name', after adding the new three-flavour channels, given in **bold** . The number between brackets is the electrical charge, useful to distinguish degenerate cases. Of course, swapping all d and u quarks gives another degenerate combination.

To extract effective masses, one cannot use the standard definition at $T = 0$,

$$m_{\text{eff}}(n_\tau) = -\log \frac{G(n_\tau + 1)}{G(n_\tau)}, \tag{2}$$

(and similarly when starting on the opposite side of the lattice), since it does not take the back walkers into account properly. This shows up as non-flat behaviour around the minimum of the correlator, see Fig. 5. Of course in the real fits, the correct equation (1) (for the case of single poles) is used. The issue is how to visualise effective masses conveniently, to judge the validity of the extracted masses.

Here we will do the algebra. We write the correlator as

$$G(n) = Ax^n + By^{N-n}, \tag{3}$$

	$I(J^P)$	PDG	Gen2	Gen2L (11/19)	Gen2L (03/20)
N	$\frac{1}{2}(\frac{1}{2}^+)$	939	1159(13)	1079(21)	1045(19)
	$\frac{1}{2}(\frac{1}{2}^-)$	1535	1778(52)	1540(51)	1581(33)
Δ	$\frac{3}{2}(\frac{3}{2}^+)$	1232	1459(58)	1447(37), 1447(46)	1479(77), 1479(33)
	$\frac{3}{2}(\frac{3}{2}^-)$	1710	2138(117)	1786(158), 1786(153)	2135(80), 2134(69)
Σ	$1(\frac{1}{2}^+)$	1193	1277(13)	1256(19)	1236(11), 1236(11)
	$1(\frac{1}{2}^-)$	1750	1823(35)	1716(41)	1736(23), 1736(23)
Λ	$0(\frac{1}{2}^+)$	1116	1248(12)	–	1176(14)
	$0(\frac{1}{2}^-)$	1405–1670	1899(66)	–	1656(23)
Σ^*	$1(\frac{3}{2}^+)$	1385	1526(32)	1520(28)	1535(49), 1345(41)
	$1(\frac{3}{2}^-)$	1670–1940	2131(62)	1956(104)	2112(62), 2323(24)
Ξ	$\frac{1}{2}(\frac{1}{2}^+)$	1318	1355(9)	1347(20)	1333(11)
	$\frac{1}{2}(\frac{1}{2}^-)$	1690–1950	1917(27)	1854(42)	1874(20)
Ξ^*	$\frac{1}{2}(\frac{3}{2}^+)$	1530	1594(24)	1612(23)	1612(49)
	$\frac{1}{2}(\frac{3}{2}^-)$	1820	2164(42)	2108(53)	2117(45)
Ω	$0(\frac{3}{2}^+)$	1672	1661(21)	1703(16)	1695(42)
	$0(\frac{3}{2}^-)$	2250	2193(30)	2233(46)	2185(45)

Table 2: Groundstate masses $m_\pm$ (in MeV) for charmless baryons ($C = 0$) in both parity sectors ($P = \pm$) in vacuum ($N_\tau = 128$ for Gen2L). The third column shows the values from the PDG. Note that in some cases there is more than one candidate in the PDG. Estimates for statistical and systematic uncertainties on Gen2 and Gen2L are included. Gen2 results are taken from Ref. [7]. When there is more than one number, channels with different u, d content are computed.

where

$$x = e^{-m_+}, \qquad y = e^{-m_-}, \tag{4}$$

and we moved to lattice units ($N = N_\tau$). Eq. (3) contains 4 unknowns, x, y, A, B. Hence we need to use 4 time slices. We write these as

$$g_0 = G(n) = Ax^n + By^{N-n}, \tag{5}$$
$$g_1 = G(n+1) = Ax^{n+1} + By^{N-n-1}, \tag{6}$$
$$g_2 = G(n+2) = Ax^{n+2} + By^{N-n-2}, \tag{7}$$
$$g_3 = G(n+3) = Ax^{n+3} + By^{N-n-3}. \tag{8}$$

This will give the effective masses at time $n_\tau = n + \frac{3}{2}$. We start by eliminating

A and B. I used the equations for $g_{0,3}$ but it should not matter. This yields

$$A = \frac{x^{-n}}{1-x^3y^3}\left(g_0 - g_3y^3\right), \qquad B = \frac{y^{3+n-N}}{1-x^3y^3}\left(g_3 - g_0x^3\right). \tag{9}$$

Substituting these in the equations for $g_{1,2}$ yields

$$g_1 = \frac{g_3y^2 + g_0x(1+xy)}{1+xy+x^2y^2}, \qquad g_2 = \frac{g_0x^2 + g_3y(1+xy)}{1+xy+x^2y^2}. \tag{10}$$

Hence to solve for x, y we have to solve

$$f_1(x,y) \equiv \left(1+xy+x^2y^2\right)g_1 - g_3y^2 - g_0x(1+xy) = 0, \tag{11}$$
$$f_2(x,y) \equiv \left(1+xy+x^2y^2\right)g_2 - g_0x^2 - g_3y(1+xy) = 0. \tag{12}$$

Surprisingly, both are quadratic equations in x and y, so we can first solve for e.g. y explicitly and then substitute the answer in the other equation. Solving $f_2(x,y) = 0$ for y yields

$$y_\pm = \frac{g_2x - g_3 \pm \sqrt{(g_3-g_2x)(g_3+3g_2x-4g_0x^3)}}{2x(g_3-g_2x)}. \tag{13}$$

We substitute these solutions back into the equation for $f_1(x,y)$, to find the equation for x only,

$$\begin{aligned} f_\pm(x) &\equiv f_1(x, y_\pm) \\ &= \frac{g_3-g_0x^3}{2x^2(g_2x-g_3)}\left(g_3 + x(g_2-2g_1x) \mp \sqrt{(g_3-g_2x)(g_3+3g_2x-4g_0x^3)}\right) \\ &= 0, \end{aligned} \tag{14}$$

There are a number of solutions to this equation. To select the correct one, note that x (and y) are real and that $0 < x, y < 1$, see Eq. (4). With a little bit of puzzling, the desired solutions are

$$x_{\rm sol} = \frac{g_1g_2 - g_0g_3 + \sqrt{(g_1g_2-g_0g_3)^2 - 4(g_1^2-g_0g_2)(g_2^2-g_1g_3)}}{2(g_1^2-g_0g_2)} \tag{15}$$

and

$$y_{\rm sol} = y_+(x_{\rm sol}), \tag{16}$$

and hence finally

$$m_+ = -\log(x_{\rm sol}), \qquad m_- = -\log(y_{\rm sol}). \tag{17}$$

This procedure is demonstrated for fake data, with two masses for both $m_\pm$ (say, groundstate and first excited state).[1] in Figs. 6, 7, for $N_\tau = 64, 32$. One can see it works and the plateaus are clearer for larger N_τ, as expected.

It is applied to real data in Figs. 8-12. Due to the square root in the analytical solution, the solution is sometimes not defined. These points are discarded. The plots show a comparison between the simple exponential ansatz and the analytical solution. A conclusion is that they agree when there is a nice plateau. The analytical solution scatters a lot, presumably since it requires 4 adjacent points to behave nicely.

[1]Explicitly the parameters are $A_1 = 1, A_2 = 0.5, B_1 = 0.7, B_2 = 0.3, m_{+1} = 0.3, m_{+2} = 0.6, m_{-1} = 0.4, m_{-2} = 0.7$.

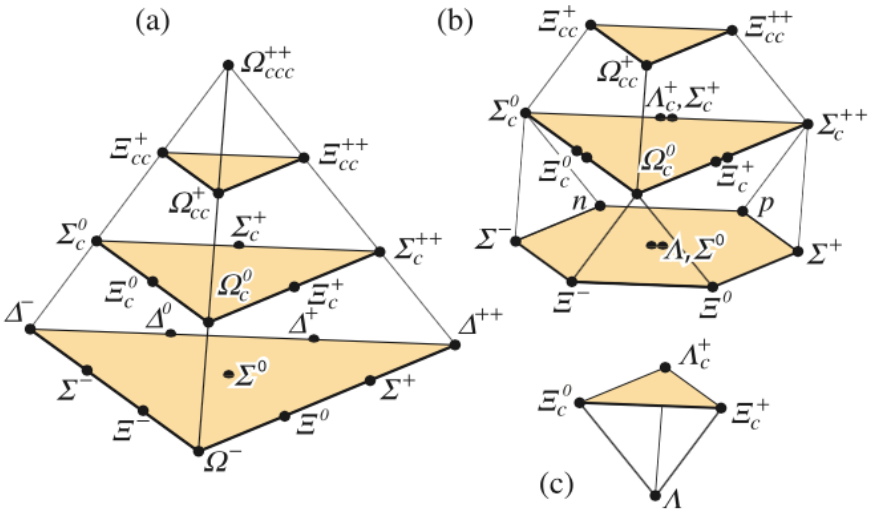

Figure 105.2: SU(4) multiplets of baryons made of u, d, s, and c quarks. (a) The 20-plet with an SU(3) decuplet on the lowest level. (b) The 20′-plet with an SU(3) octet on the lowest level. (c) The $\bar{4}$-plet. Note that here and in Fig. 105.3, but not in Fig. 105.1, each charge state is shown separately.

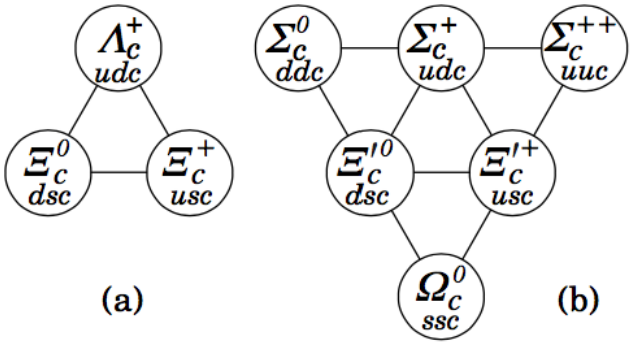

Figure 105.3: The SU(3) multiplets on the second level of the SU(4) multiplet of Fig. 105.2(b). The Λ_c and Ξ_c tabbed with closed circles in Fig. 105.1(a) complete a $J^P = 1/2^+$ SU(3) $\bar{3}$-plet, as in (a) here. The Σ_c, Ξ_c, and Ω_c tabbed with open circles in Fig. 105.1(a) complete a $J^P = 1/2^+$ SU(3) 6-plet, as in (b) here. Together the nine particles complete the charm = +1 level of a $J^P = 1/2^+$ SU(4) 20′-plet, as in Fig. 105.2(b).

Figure 1: From [3].

	$I(J^P)$	PDG	Gen2	Gen2L (11/19)	Gen2L (03/20)
Λ_c	$0(\frac{1}{2}^+)$	2286	–	–	2307(11)
	$0(\frac{1}{2}^-)$	2595	–	–	2836(17)
Σ_c	$1(\frac{1}{2}^+)$	2455	–	2495(112)	2467(10), 2467(10)
	$1(?^?/\frac{1}{2}^-)$	2800	–	2883(30)	2882(15), 2882(15)
Σ_c	$1(\frac{3}{2}^+)$	2520	–	2591(25)	2596(24), 2539(20)
	$1(\frac{3}{2}^-)$		–	2950(64)	2893(36), 2951(31)
Ξ_c	$\frac{1}{2}(\frac{1}{2}^+)$	2468	–	–	2449(8)
	$\frac{1}{2}(\frac{1}{2}^-)$	2790	–	–	2943(17)
Ξ_c'	$\frac{1}{2}(\frac{1}{2}^+)$	2578	–	–	2562(9)
	$\frac{1}{2}(\frac{1}{2}^-)$		–	–	2978(16)
Ξ_c	$\frac{1}{2}(\frac{3}{2}^+)$	2646	–	–	2620(21)
	$\frac{1}{2}(\frac{3}{2}^-)$	2815	–	–	3048(27)
Ω_c	$0(\frac{1}{2}^+)$	2695	–	2672(10)	2655(8)
	$0(\frac{1}{2}^-)$		–	3077(31)	3076(15)
Ω_c	$0(\frac{3}{2}^+)$	2770	–	2754(10)	2738(26)
	$0(\frac{3}{2}^-)$		–	3163(45)	3109(31)
Ω_c	$?(?^?)$	3000			
Ξ_{cc}	$\frac{1}{2}(\frac{1}{2}^+)$	3621	–	3584(8)	3571(5)
	$\frac{1}{2}(\frac{1}{2}^-)$		–	4015(33)	4033(18)
Ξ_{cc}	$\frac{1}{2}(\frac{3}{2}^+)$		–	3684(11)	3671(19)
	$\frac{1}{2}(\frac{3}{2}^-)$		–	4044(30)	4009(30)
Ω_{cc}	$0(\frac{1}{2}^+)$		–	3670(6)	3660(5)
	$0(\frac{1}{2}^-)$		–	4101(27)	4108(14)
Ω_{cc}	$0(\frac{3}{2}^+)$		–	3758(10)	3737(17)
	$0(\frac{3}{2}^-)$		–	4141(35)	4116(25)
Ω_{ccc}	$0(\frac{3}{2}^+)$		–	4725(7)	4706(11)
	$0(\frac{3}{2}^-)$		–	5208(57)	5126(50)

Table 3: As above, for charmed baryons ($C \neq 0$). Not all states have been found experimentally, nor have all quantum numbers been determined. $\Omega_c(3000)$ might be identified with the $P = -1$ state, for both $J = \frac{1}{2}, \frac{3}{2}$. Note that for the $\Xi_{cc}(3621)$ the PDG does not list quantum numbers; we assume it is $\frac{1}{2}(\frac{1}{2}^+)$.

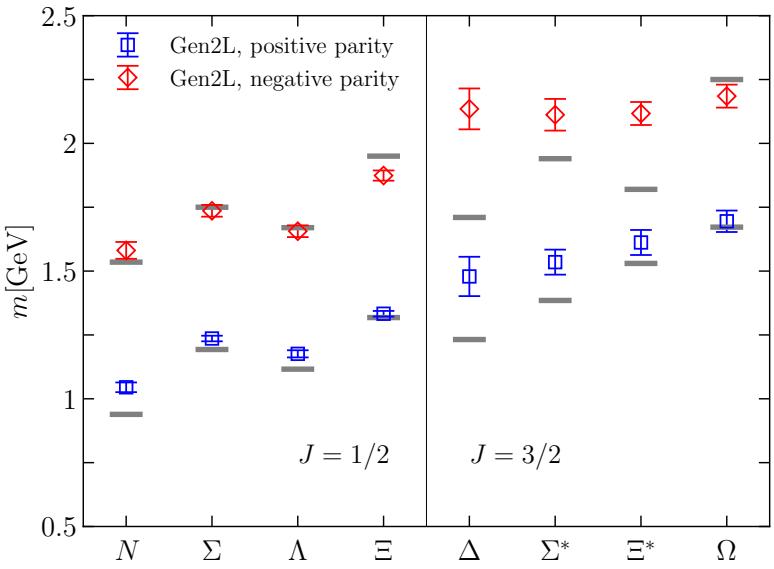

Figure 2: Spectrum at $T = 0$ for light baryons, for Gen2L. PDG results are indicated with the horizontal lines.

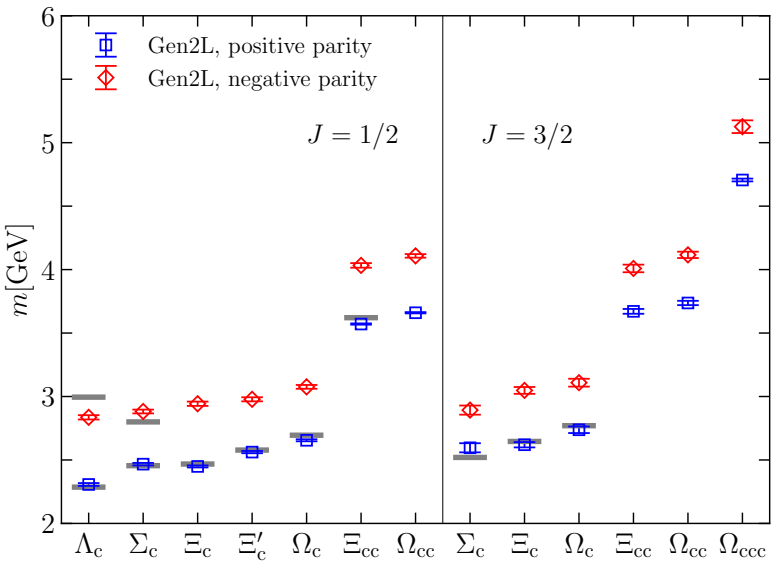

Figure 3: As above, for charmed baryons.

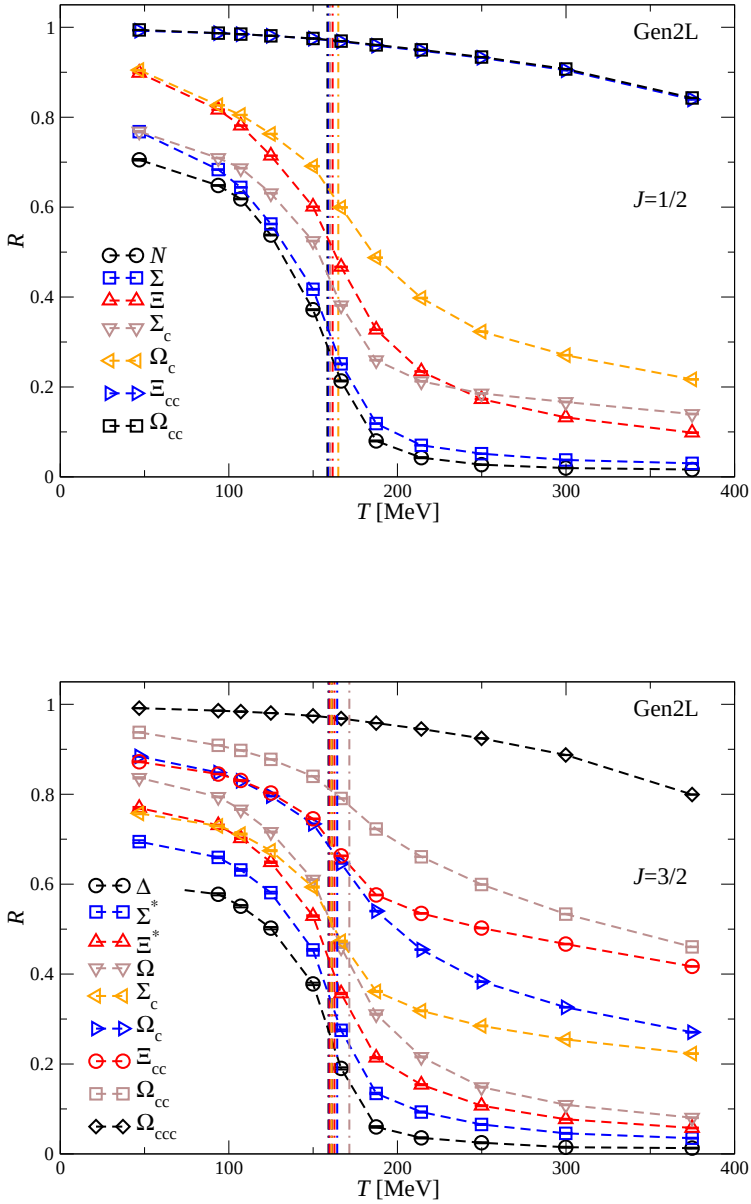

Figure 4: Baryon R paramater in $J = \frac{1}{2}$ (top) and $J = \frac{3}{2}$ (bottom) baryonic channels. The vertical lines indicate the inflection points.

spin	particle	T_{inf} [MeV]
$\frac{1}{2}$	N	158.514
	Σ	159.124
	Ξ	161.560
	Σ_c	159.998
	Ω_c	164.917
	Ξ_{cc}	–
	Ω_{cc}	–
$\frac{3}{2}$	Δ	159.124
	Σ^*	159.530
	Ξ^*	159.733
	Ω	161.154
	Σ_c	160.982
	Ω_c	164.262
	Ξ_{cc}	162.622
	Ω_{cc}	171.477
	Ω_{ccc}	–

Table 4: Temperature of the inflection point in the R parameter, labelled by channel.

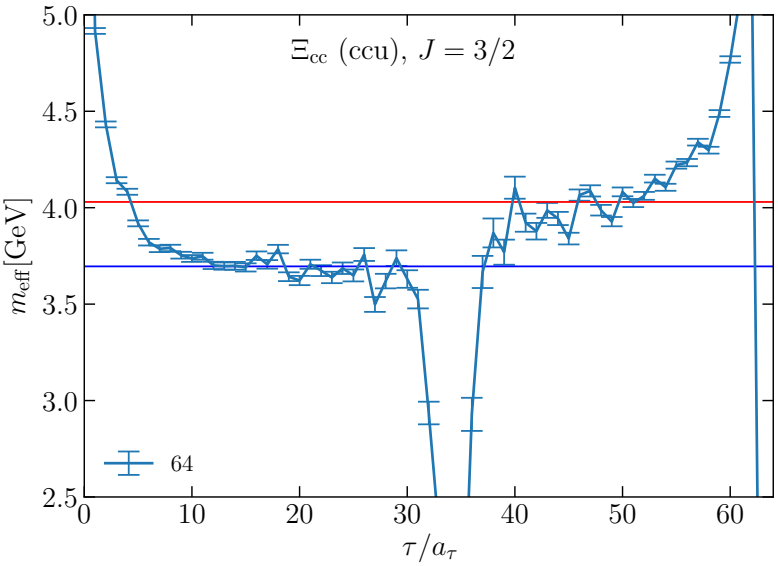

Figure 5: Effective mass, as defined in Eq. (2), for 32-Xi_cc-ccu, at $N_\tau = 64$. Horizontal lines are the used values.

channel	$n_0 = 1$	2	3	4	5	6
N (uud), $J = 1/2$	158.03	157.70	157.37	156.72	156.06	155.08
Σ (uus), $J = 1/2$	158.69	158.69	158.36	158.36	158.03	157.70
Σ (uds), $J = 1/2$	158.69	158.36	158.36	158.03	158.03	157.70
Λ (uds), $J = 1/2$	156.72	156.39	156.39	155.73	154.75	153.11
Ξ (ssu), $J = 1/2$	160.00	160.00	160.00	159.67	159.67	159.34
Δ (uuu), $J = 3/2$	158.36	158.03	157.70	157.37	157.05	156.72
Δ (uud), $J = 3/2$	158.36	158.03	157.70	157.37	157.05	156.72
Σ^* (uus), $J = 3/2$	158.36	158.03	158.03	157.70	157.37	157.05
Σ^* (uds), $J = 3/2$	158.03	158.03	157.70	157.37	157.05	157.05
Ξ^* (ssu), $J = 3/2$	158.69	158.69	158.36	158.36	158.03	157.70
Ω (sss), $J = 3/2$	160.00	160.00	160.00	159.67	159.34	159.01
Λ_c (udc), $J = 1/2$	174.43	175.41	175.74	175.74	176.07	176.40
Σ_c (uuc), $J = 1/2$	160.00	160.00	160.00	159.67	159.67	159.67
Σ_c (udc), $J = 1/2$	160.00	159.67	159.67	159.67	159.34	159.34
Ξ_c (usc), $J = 1/2$	159.67	159.67	160.00	160.00	160.33	160.65
Ξ'_c (usc), $J = 1/2$	160.33	160.33	160.33	160.33	160.33	160.33
Ω_c (ssc), $J = 1/2$	162.29	162.62	162.62	162.29	162.62	162.62
Ξ_{cc} (ccu), $J = 1/2$	374.81	374.81	374.81	374.81	357.10	311.52
Ω_{cc} (ccs), $J = 1/2$	374.81	374.81	374.81	374.81	354.81	311.84
Σ_c (uuc), $J = 3/2$	159.01	159.01	159.01	158.69	158.69	158.69
Σ_c (udc), $J = 3/2$	159.01	159.01	158.69	158.69	158.36	158.36
Ξ_c (usc), $J = 3/2$	159.34	159.34	159.34	159.01	159.01	159.01
Ω_c (ssc), $J = 3/2$	161.31	161.64	161.64	161.64	161.64	161.97
Ξ_{cc} (ccu), $J = 3/2$	160.00	160.33	160.33	160.33	160.33	160.33
Ω_{cc} (ccs), $J = 3/2$	162.29	162.62	162.95	162.95	163.61	196.07
Ω_{ccc} (ccc), $J = 3/2$	374.81	374.81	374.81	374.81	319.39	298.73

Table 5: Temperature of the inflection point in the R parameter, labelled by channel.

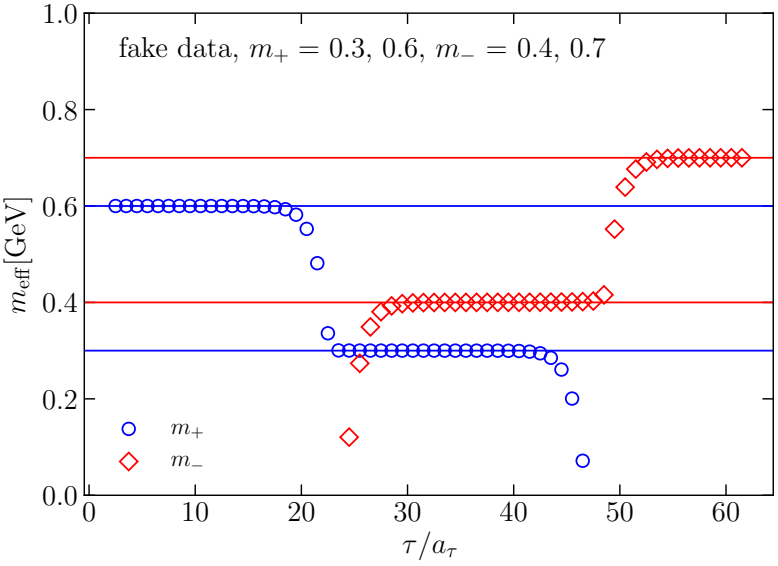

Figure 6: Effective masses for fake data, using the analytical solution, for $N_\tau = 64$.

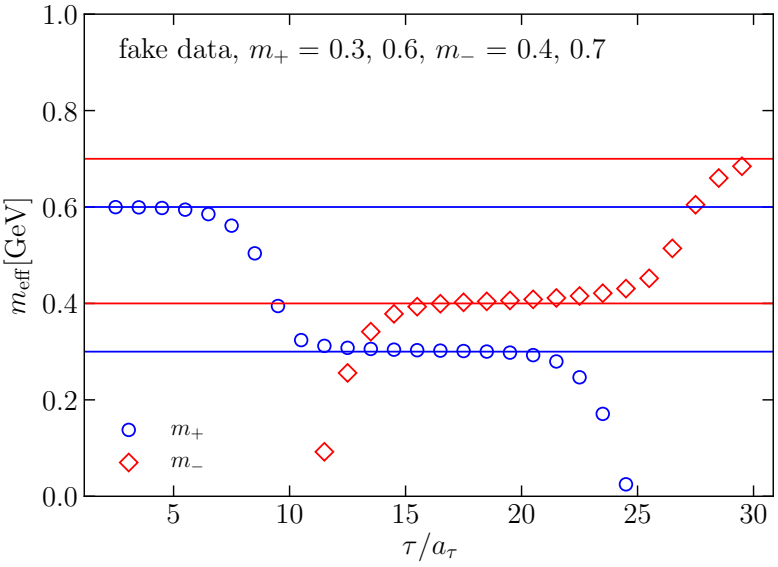

Figure 7: Effective masses for fake data, using the analytical solution, for $N_\tau = 32$.

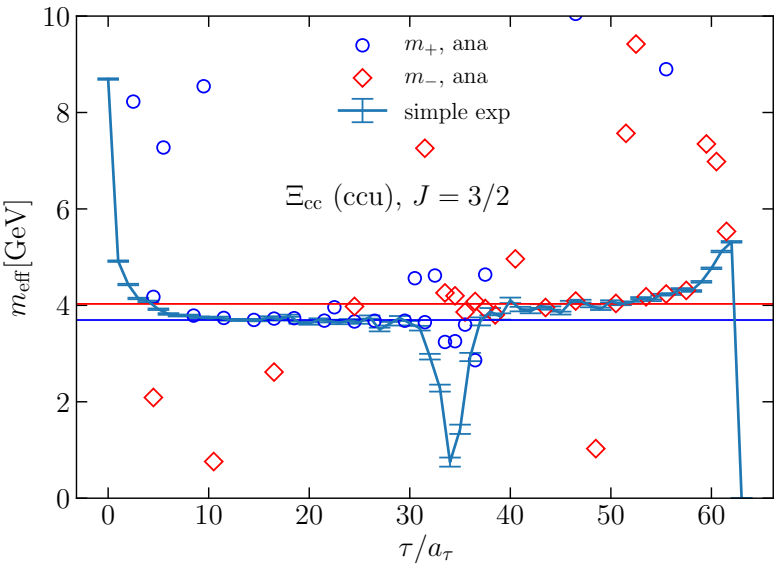

Figure 8: Comparison between effective masses from simple exponentials and from the analytical solution, for 32-Xi_cc-ccu and $N_\tau = 64$.

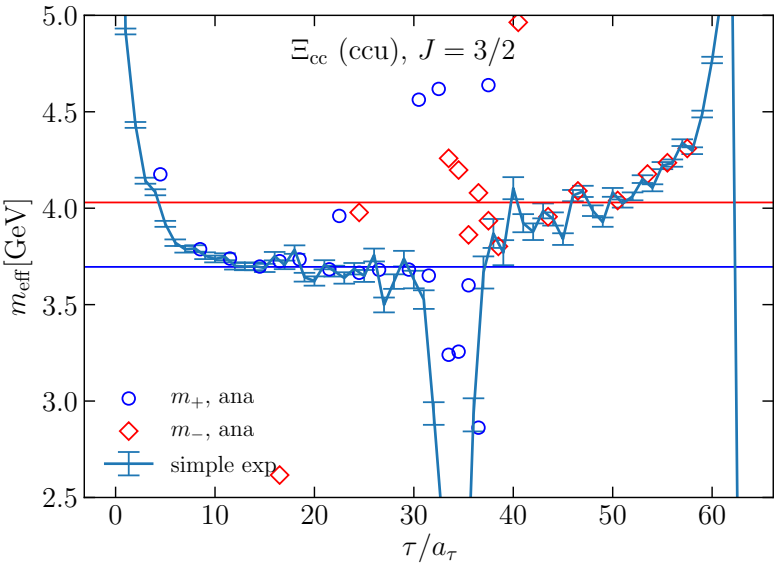

Figure 9: As above, zoomed in.

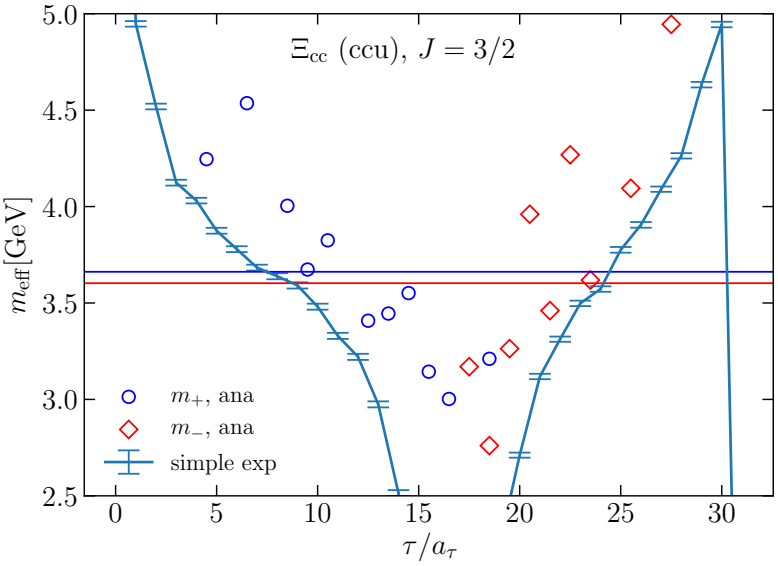

Figure 10: As above, for $N_\tau = 32$.

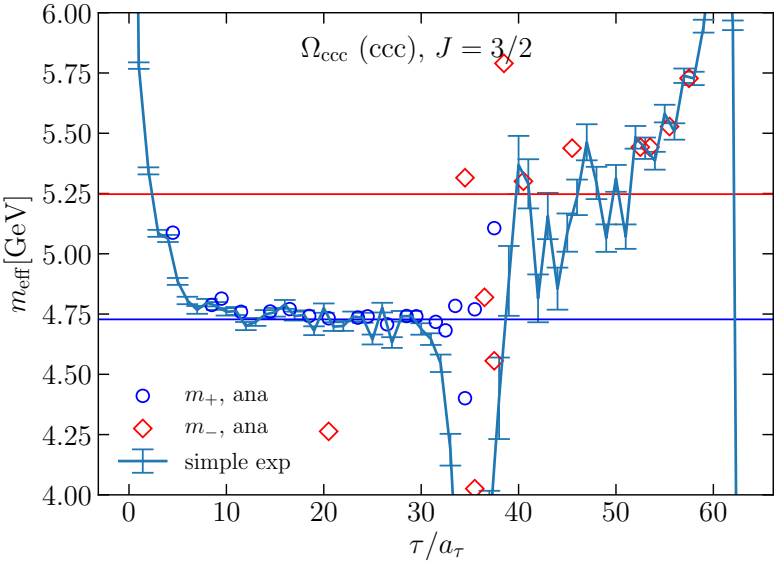

Figure 11: As above, for 32-Omega_ccc-ccc and $N_\tau = 64$.

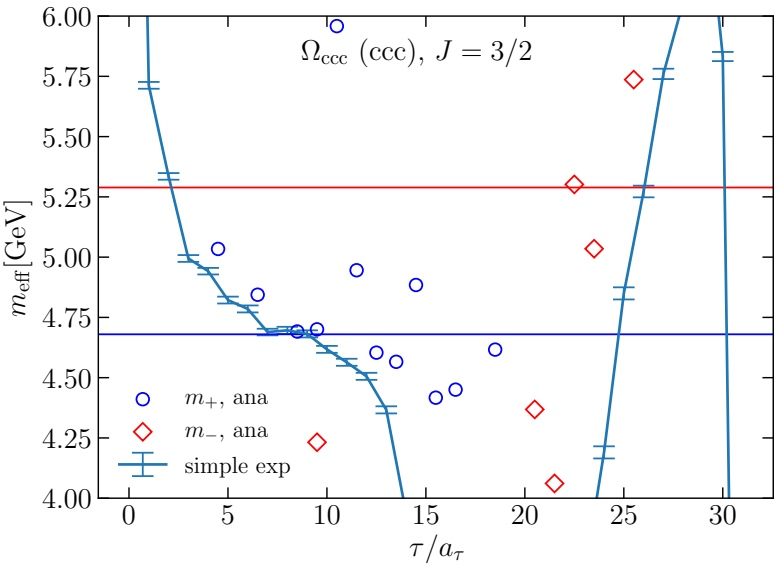

Figure 12: As above, for 32-Omega_ccc-ccc and $N_\tau = 32$.

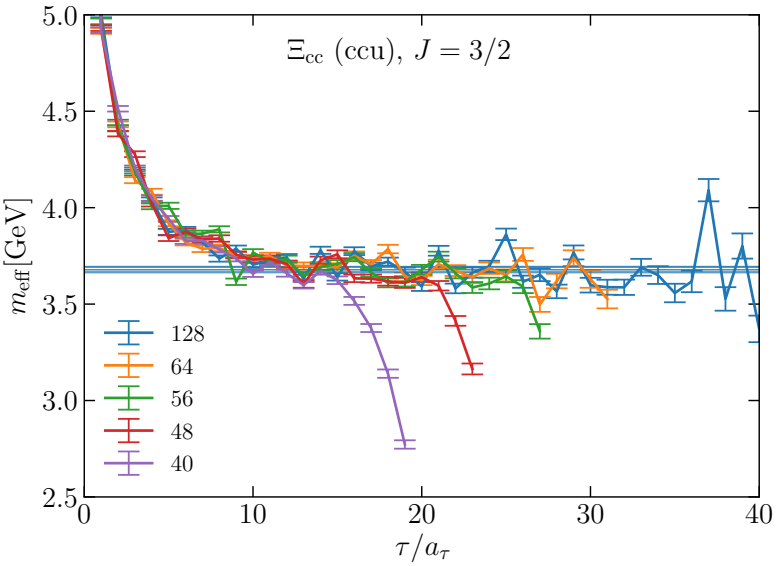

Figure 13: Effective mass for positive parity side, as defined in Eq. (2), for 32-Xi_cc-ccu, for several N_τ values.

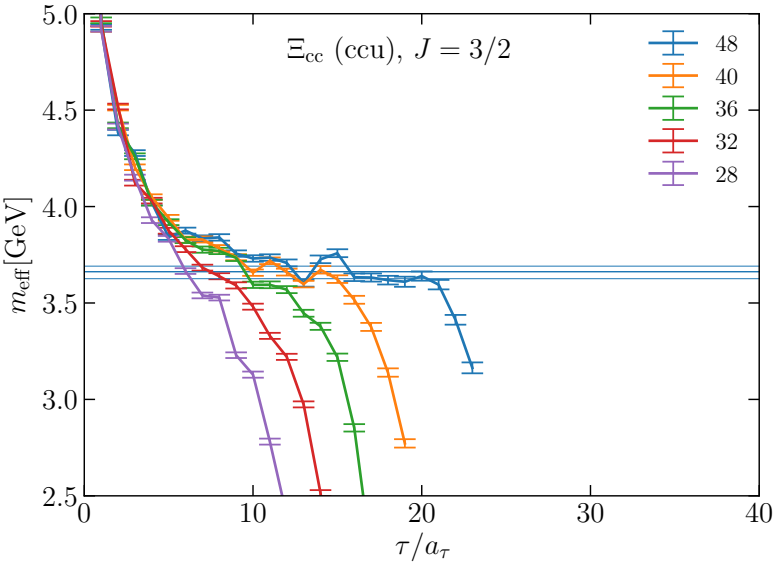

Figure 14: As above.

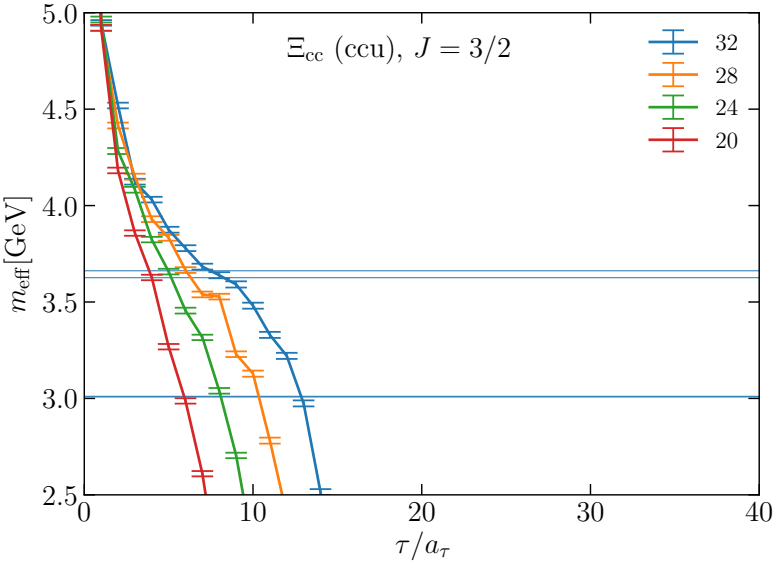

Figure 15: As above.

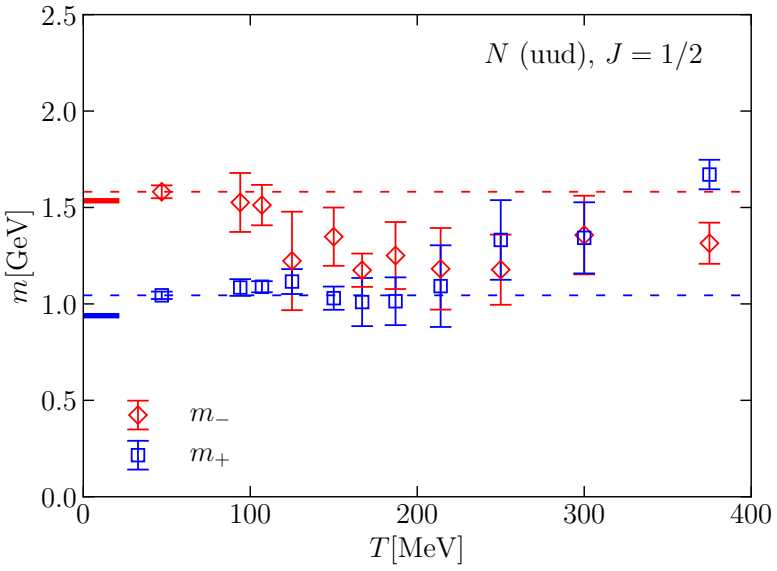

Figure 16: T dependence of the mass of 12-Nucleon-uud. The dashed lines are meant to guide the eye; the stubs on the left are the PDG values.

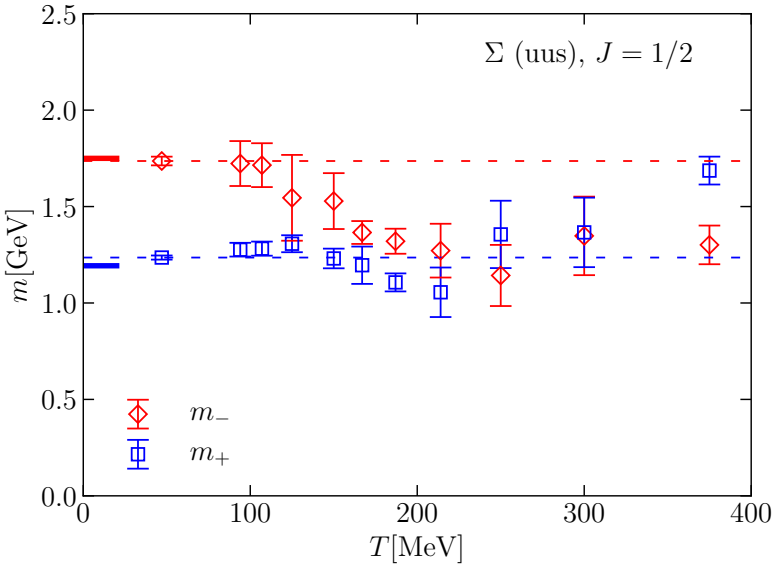

Figure 17: As above, for 12-Sigma-uus.

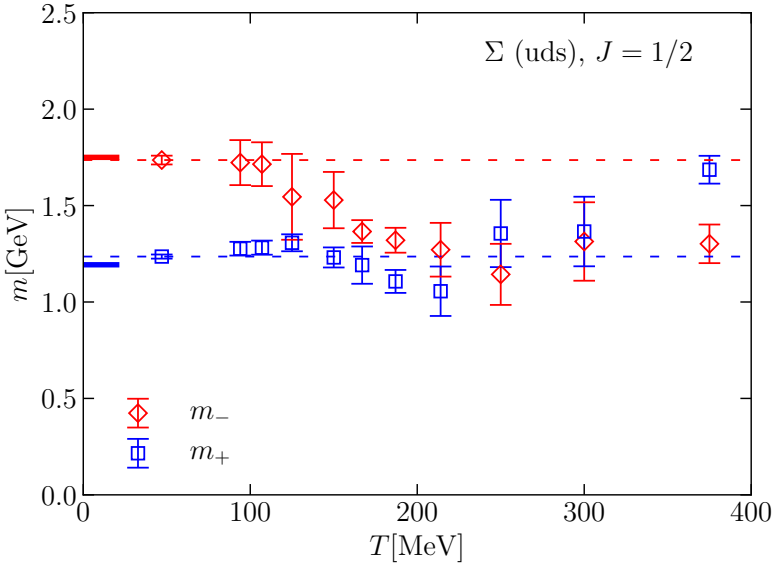

Figure 18: As above, for 12-Sigma-uds.

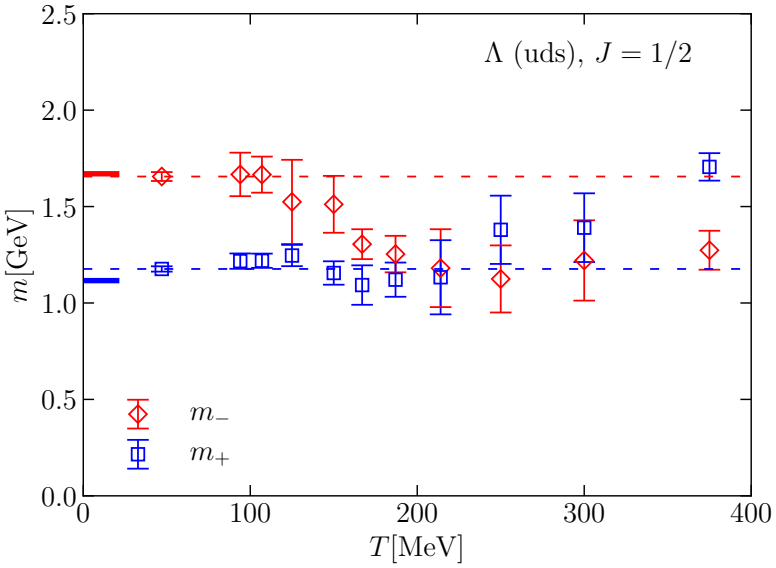

Figure 19: As above, for 12-Lambda-uds.

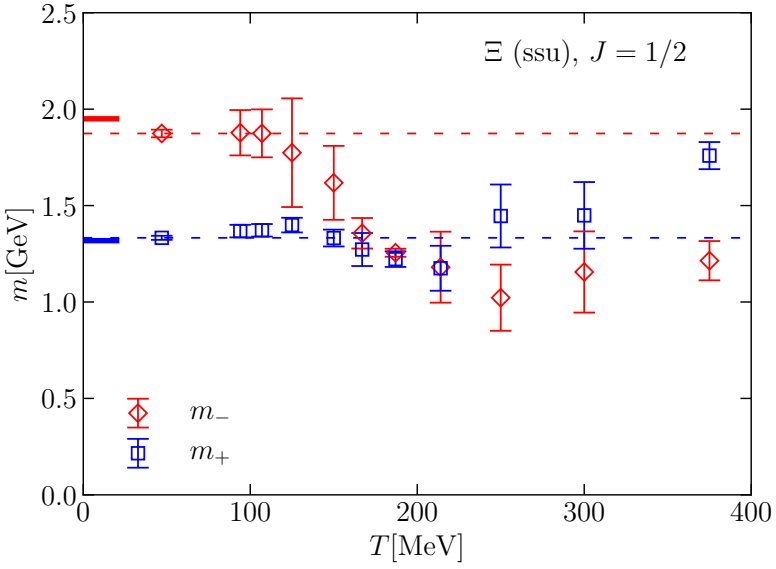

Figure 20: As above, for 12-Xi-ssu.

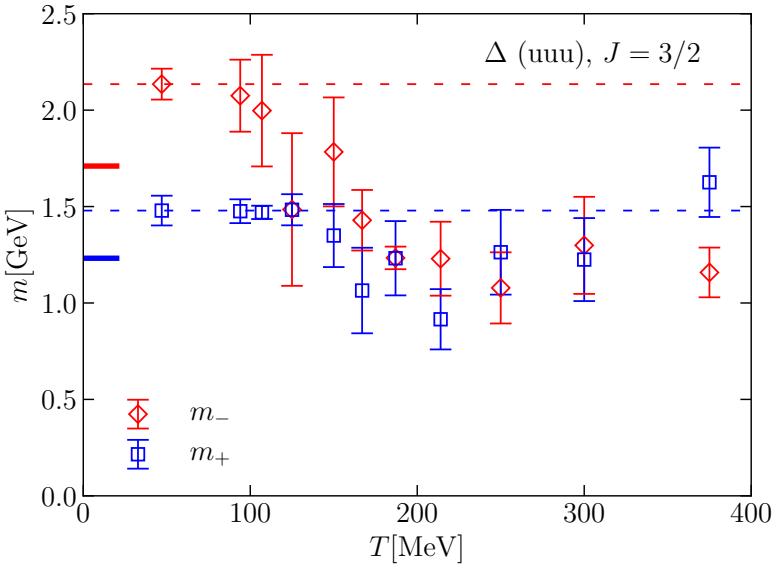

Figure 21: As above, for 32-Delta-uuu.

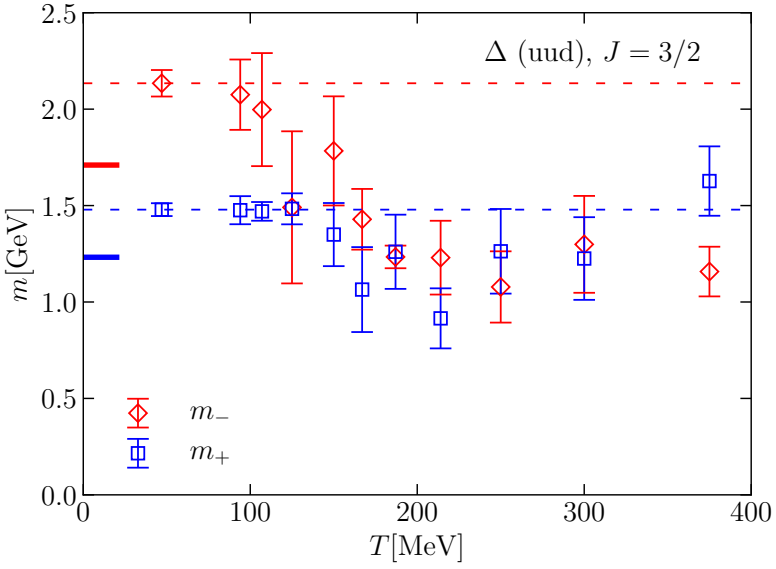

Figure 22: As above, for 32-Delta-uud.

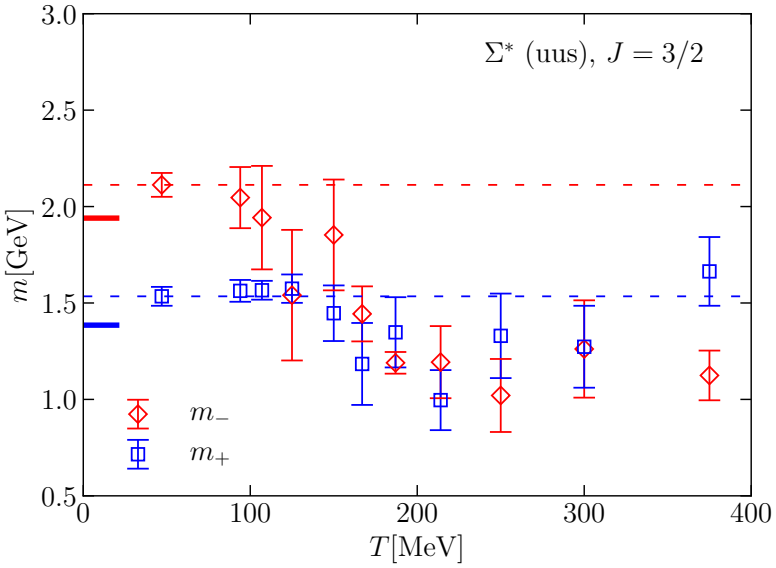

Figure 23: As above, for 32-Sigma-star-uus.

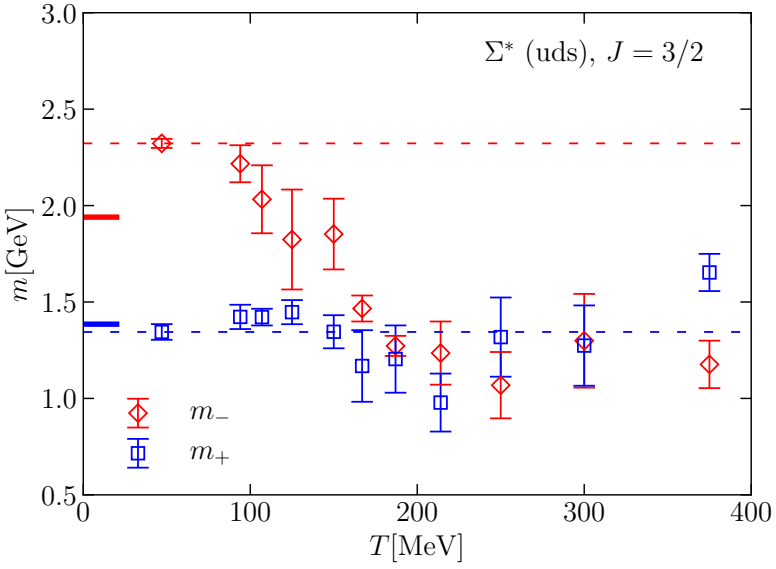

Figure 24: As above, for 32-Sigma-star-uds.

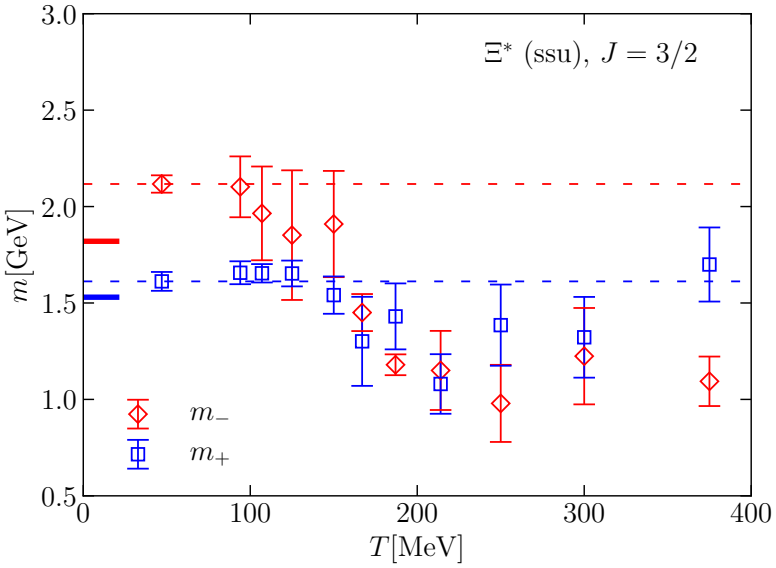

Figure 25: As above, for 32-Xi-star-ssu.

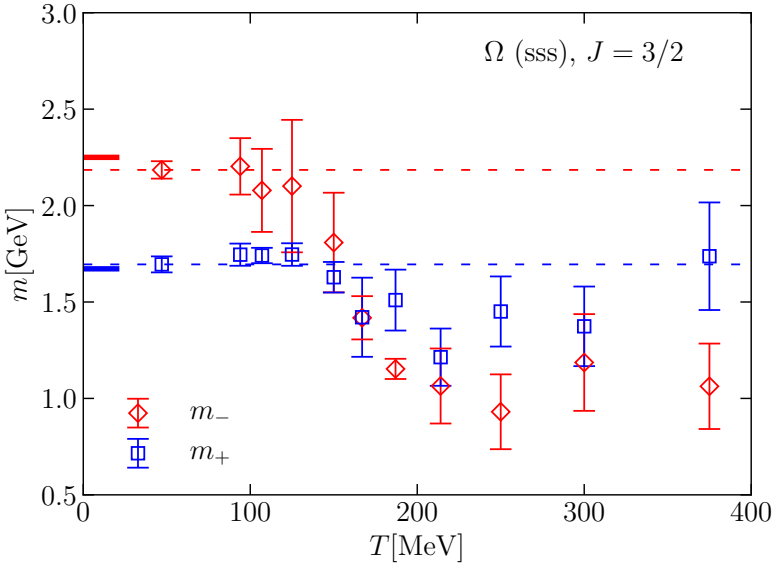

Figure 26: As above, for 32-Omega-sss.

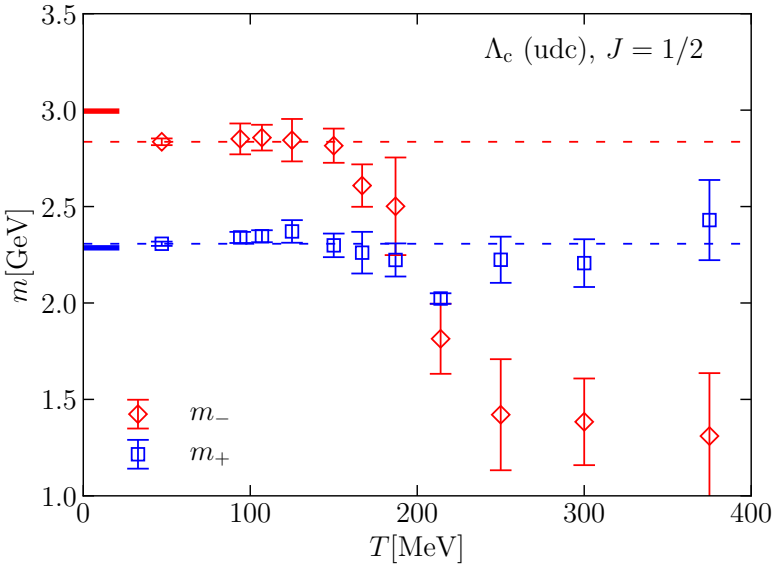

Figure 27: As above, for 12-Lambda_c-udc.

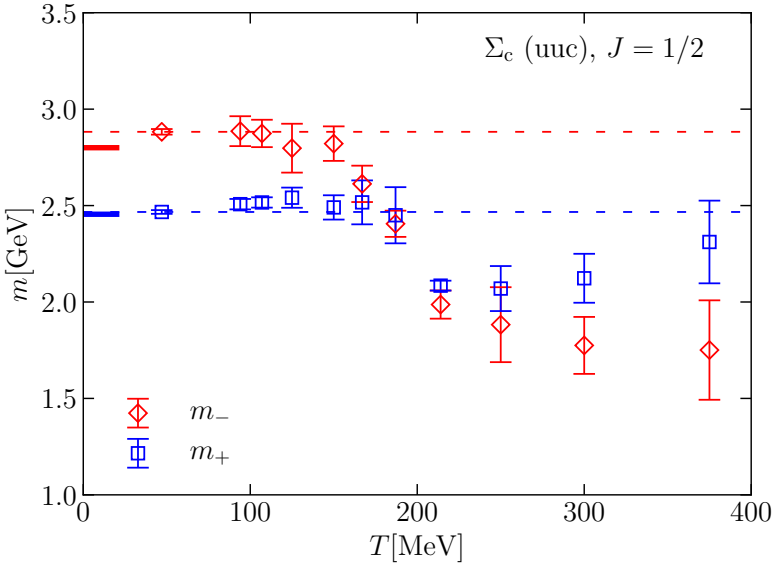

Figure 28: As above, for 12-Sigma_c-uuc.

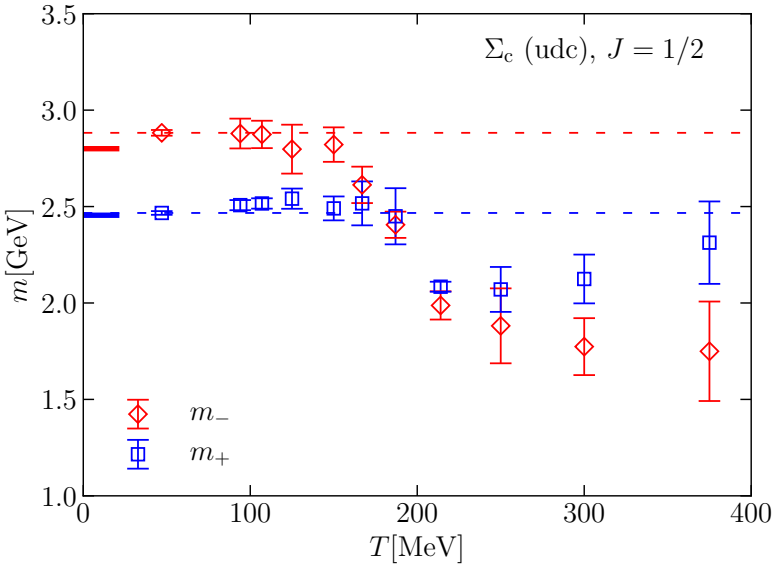

Figure 29: As above, for 12-Sigma_c-udc.

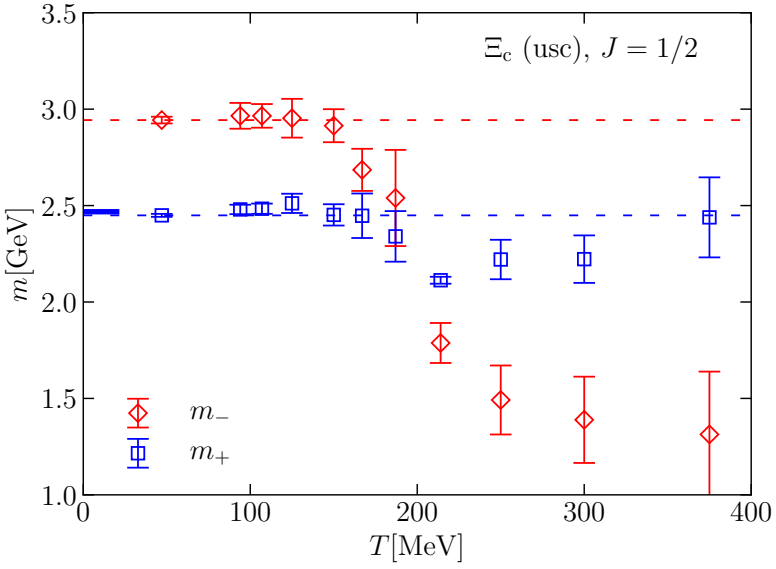

Figure 30: As above, for 12-Xi_c-usc.

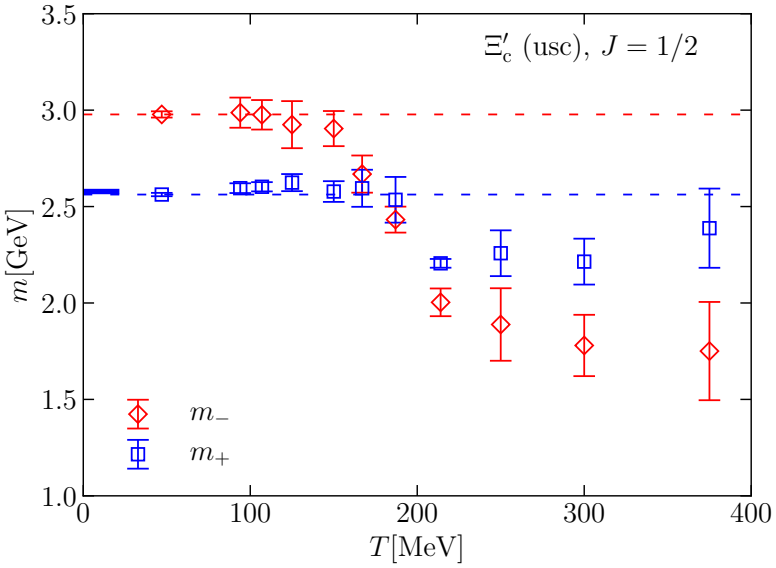

Figure 31: As above, for 12-Xi_c-prime-usc.

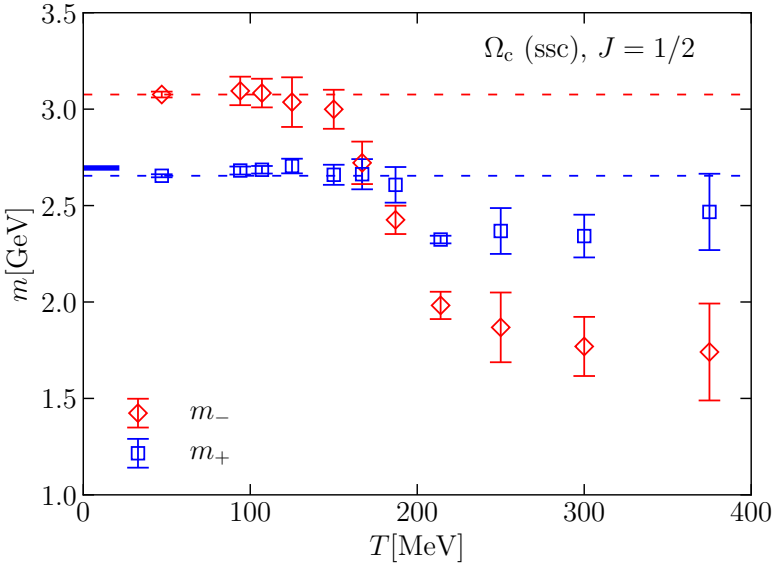

Figure 32: As above, for 12-Omega_c-ssc.

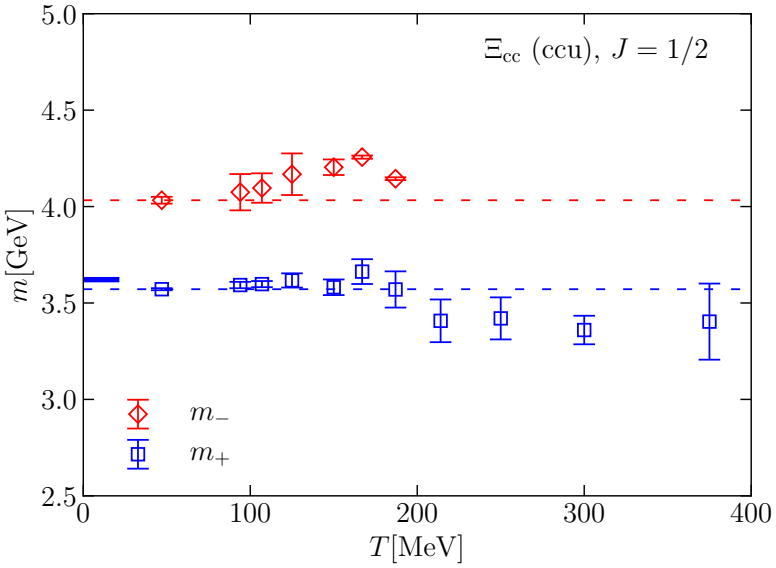

Figure 33: As above, for 12-Xi_cc-ccu.

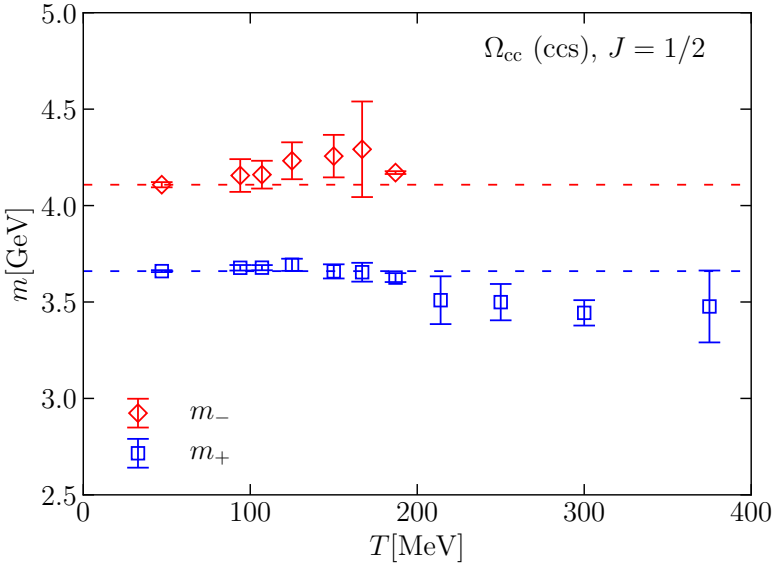

Figure 34: As above, for 12-Omega_cc-ccs.

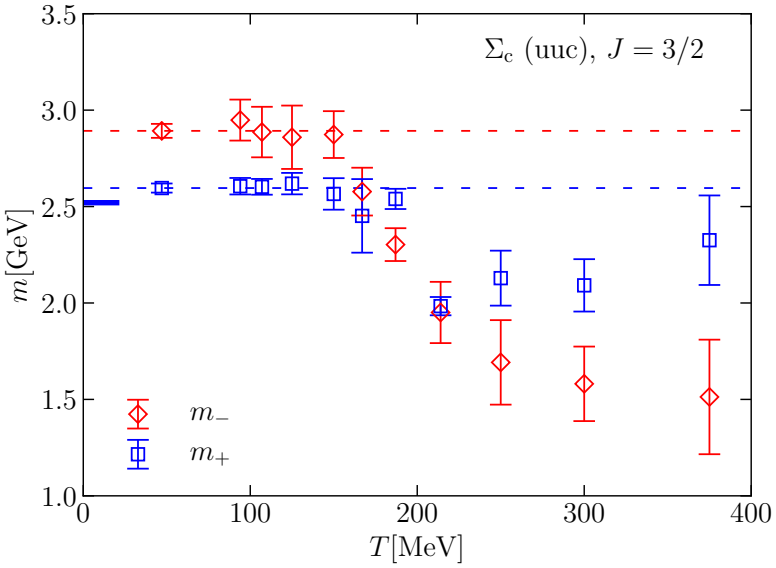

Figure 35: As above, for 32-Sigma_c-uuc.

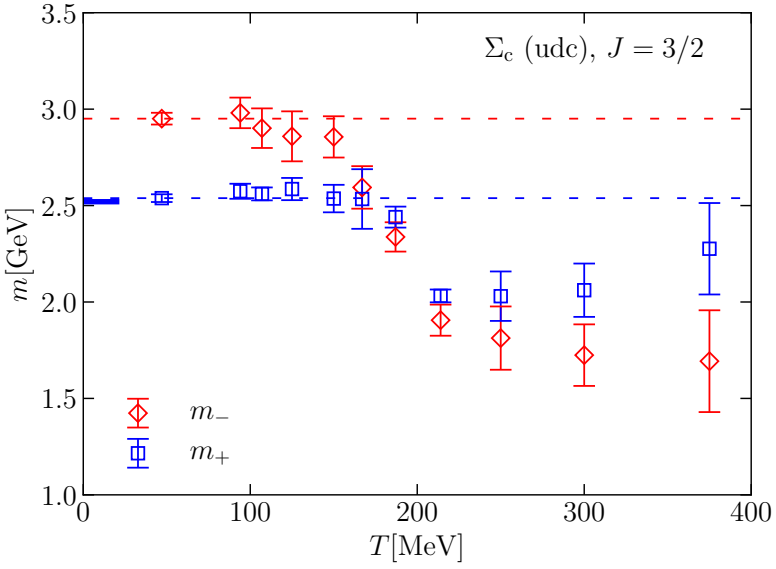

Figure 36: As above, for 32-Sigma_c-udc.

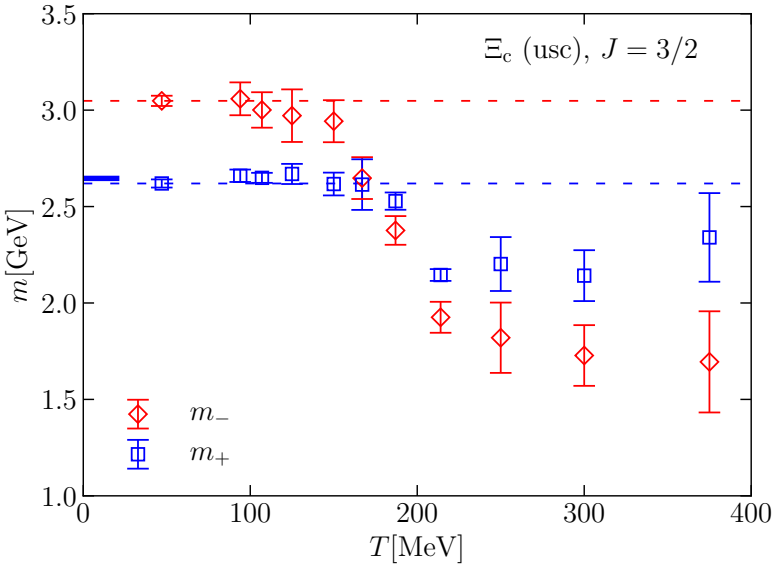

Figure 37: As above, for 32-Xi_c-usc.

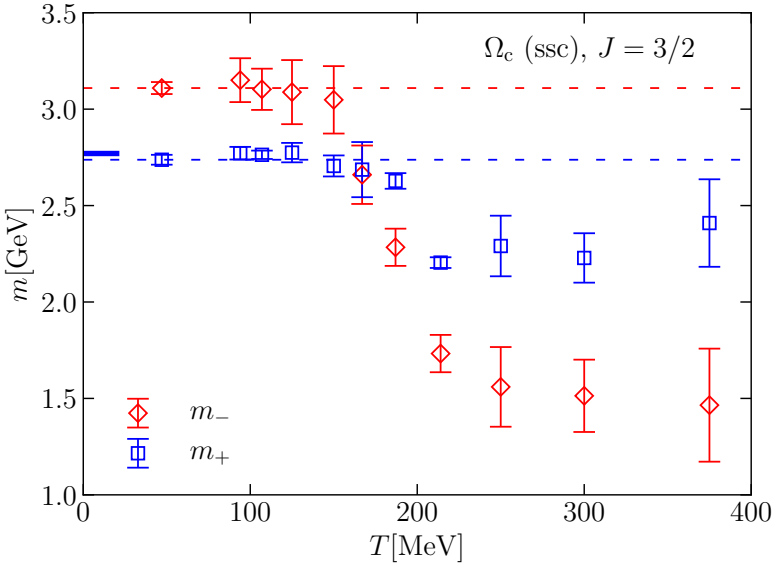

Figure 38: As above, for 32-Omega_c-ssc.

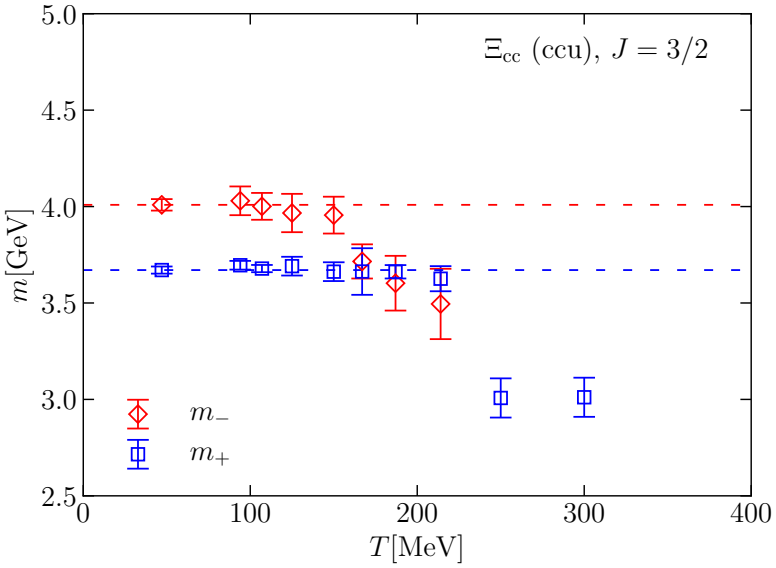

Figure 39: As above, for 32-Xi_cc-ccu.

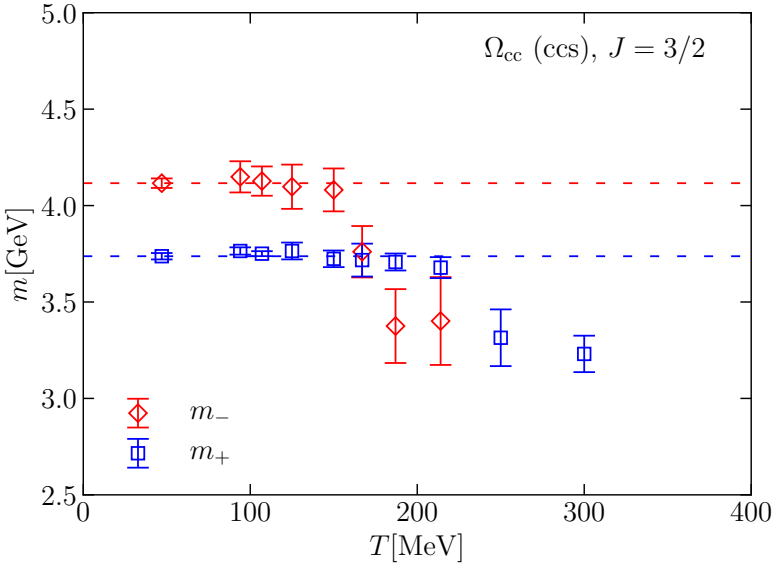

Figure 40: As above, for 32-Omega_cc-ccs.

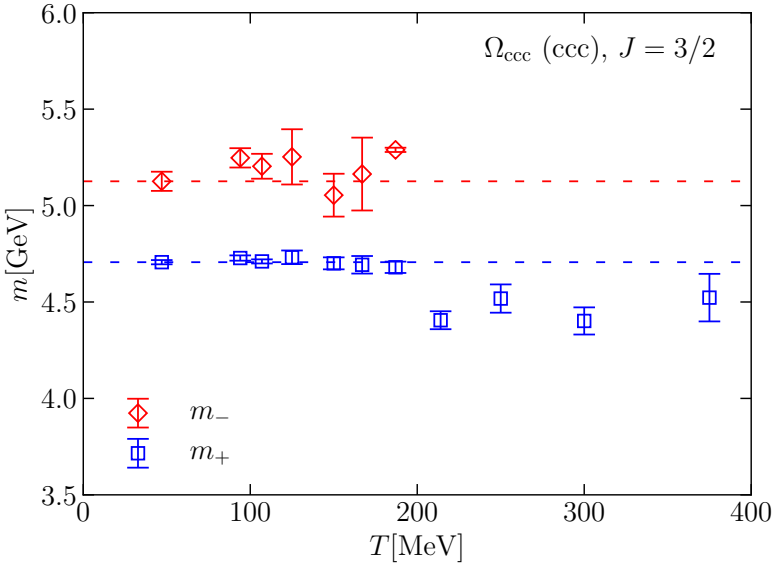

Figure 41: As above, for 32-Omega_ccc-ccc.

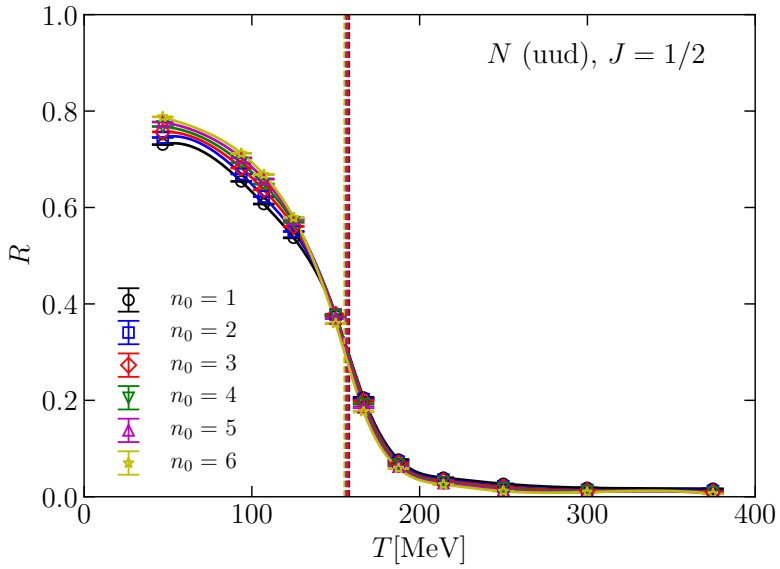

Figure 42: T dependence of R parameter, for 6 starting points $n_0 = \tau_0/a_\tau = 1 - -6$, for 12-Nucleon-uud. The data points are connected by cubic splines. The vertical dashed lines indicate the inflection point.

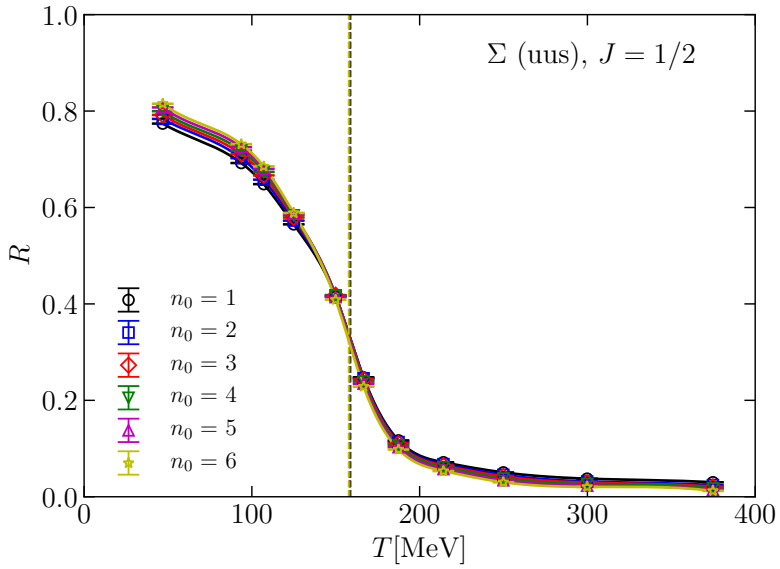

Figure 43: As above, for 12-Sigma-uus.

References

[1] https://en.wikipedia.org/wiki/Charmed_baryon

[2] M. Tanabashi *et al.* [Particle Data Group], Phys. Rev. D **98** (2018) no.3, 030001.

[3] 105. Charmed Baryons - PDG http://pdg.lbl.gov/pdg.lbl.gov reviews rpp2018-rev-charmed-baryons

[4] CHARMED BARYONS ($C = +1$) http://pdg.lbl.gov tables rpp2019-tab-baryons-Charm

[5] CHARMED BARYONS ($C = +2$) http://pdg.lbl.gov tables rpp2018-tab-baryons-charm-doubly

[6] X. Yao and B. Müller, Phys. Rev. D **97** (2018) no.7, 074003 [arXiv:1801.02652 [hep-ph]].

[7] G. Aarts, C. Allton, D. De Boni and B. Jäger, Phys. Rev. D **99** (2019) no.7, 074503 [arXiv:1812.07393 [hep-lat]].

[8] C. Alexandrou and C. Kallidonis, Phys. Rev. D **96** (2017) no.3, 034511 doi:10.1103/PhysRevD.96.034511 [arXiv:1704.02647 [hep-lat]].

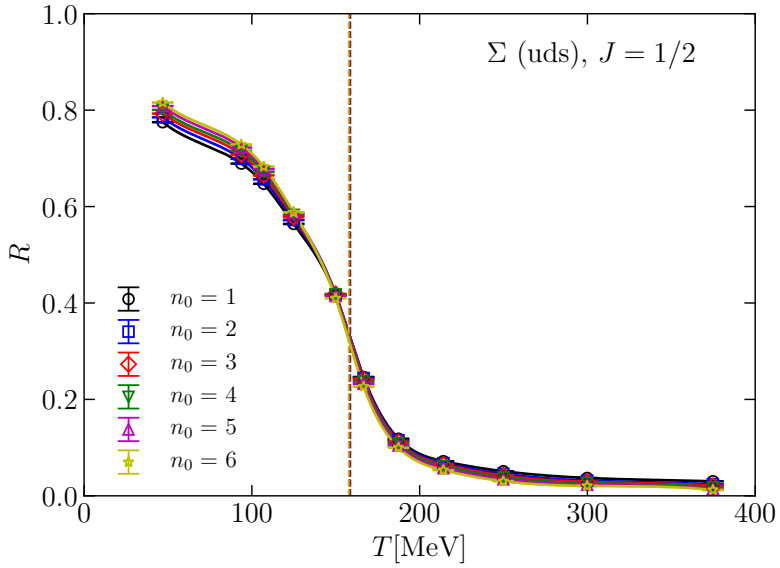

Figure 44: As above, for 12-Sigma-uds.

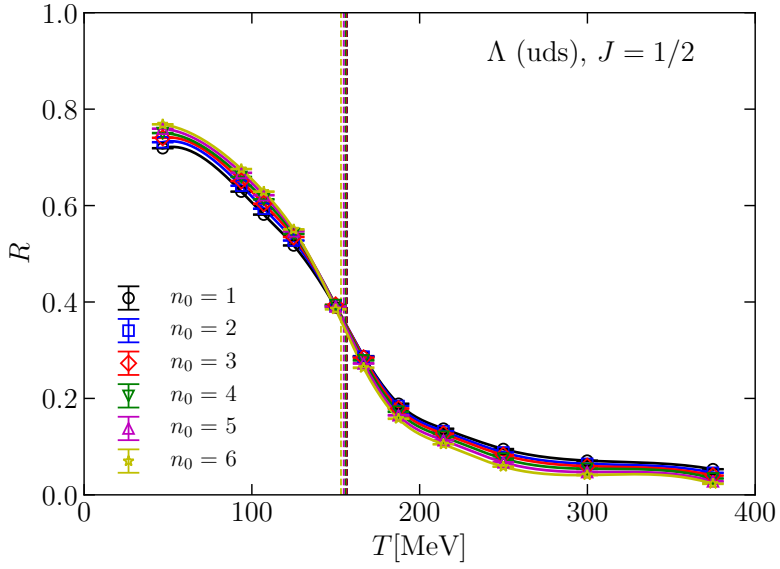

Figure 45: As above, for 12-Lambda-uds.

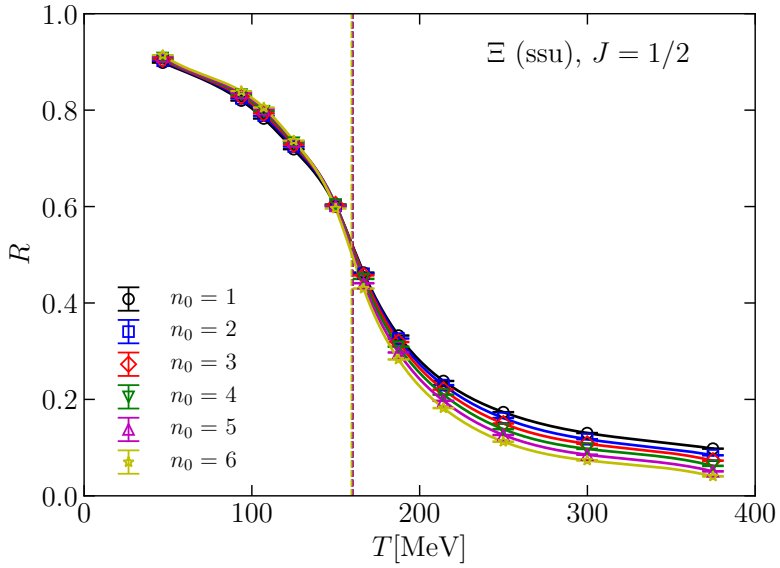

Figure 46: As above, for 12-Xi-ssu.

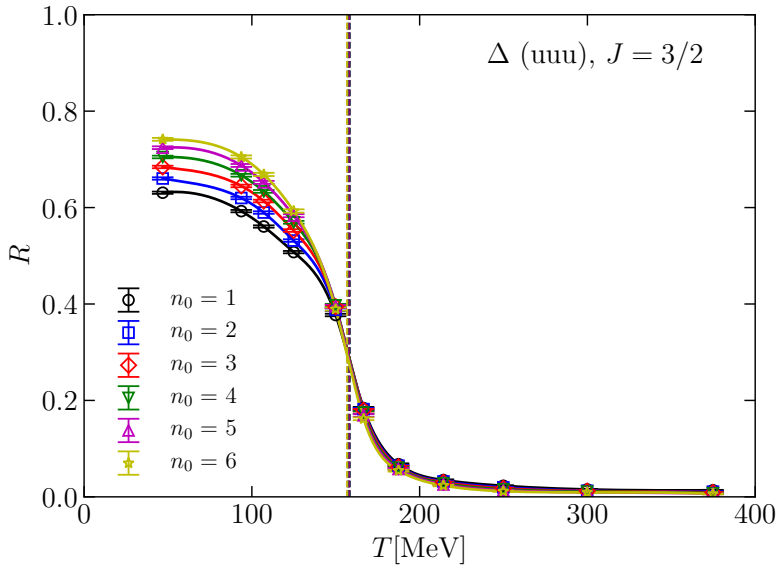

Figure 47: As above, for 32-Delta-uuu.

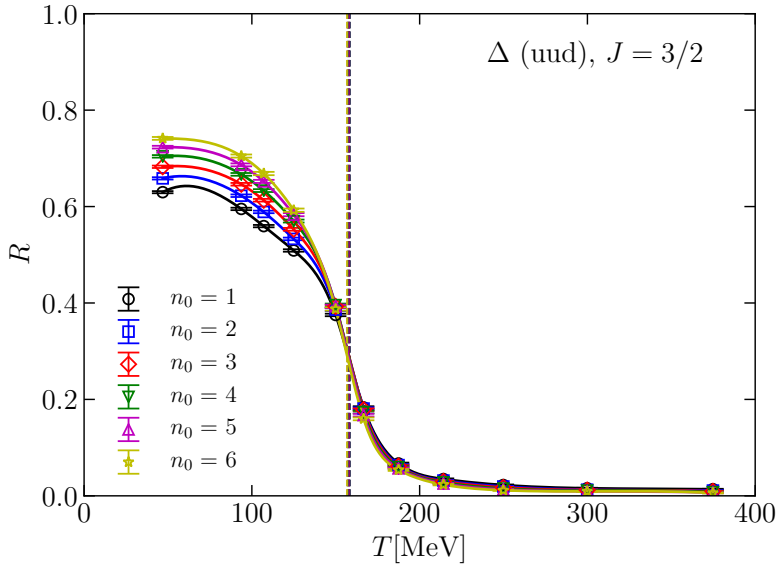

Figure 48: As above, for 32-Delta-uud.

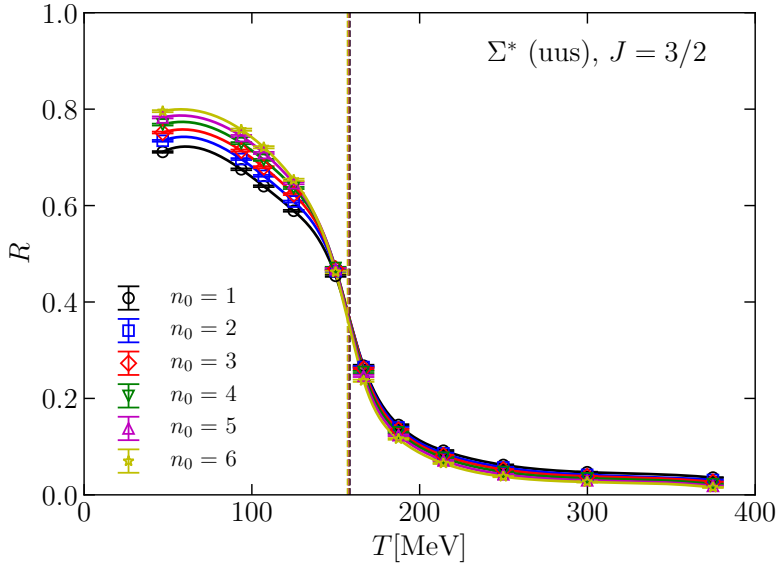

Figure 49: As above, for 32-Sigma-star-uus.

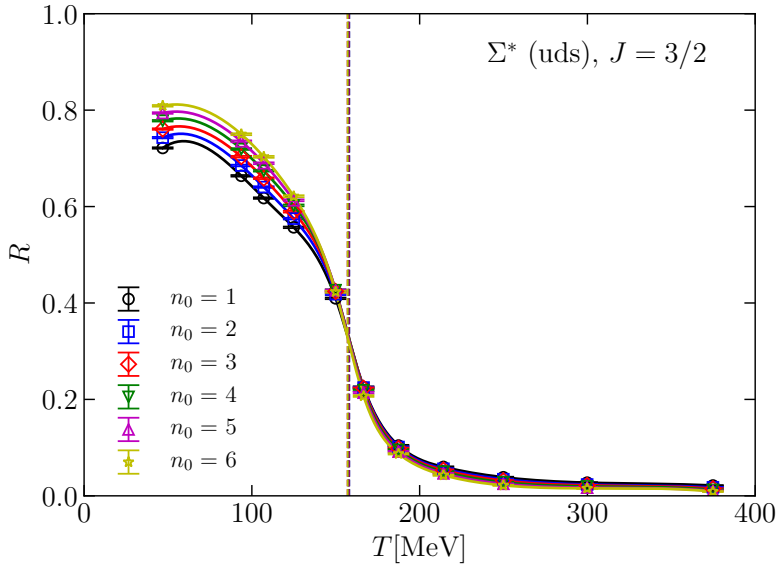

Figure 50: As above, for 32-Sigma-star-uds.

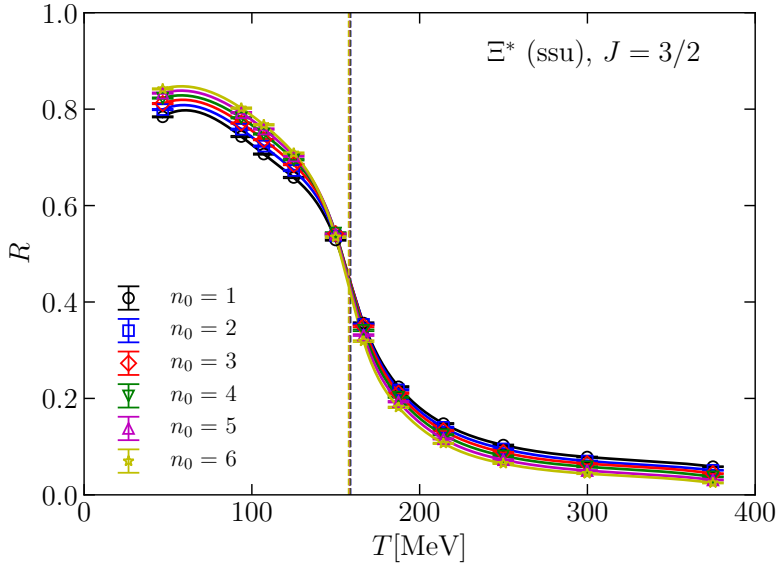

Figure 51: As above, for 32-Xi-star-ssu.

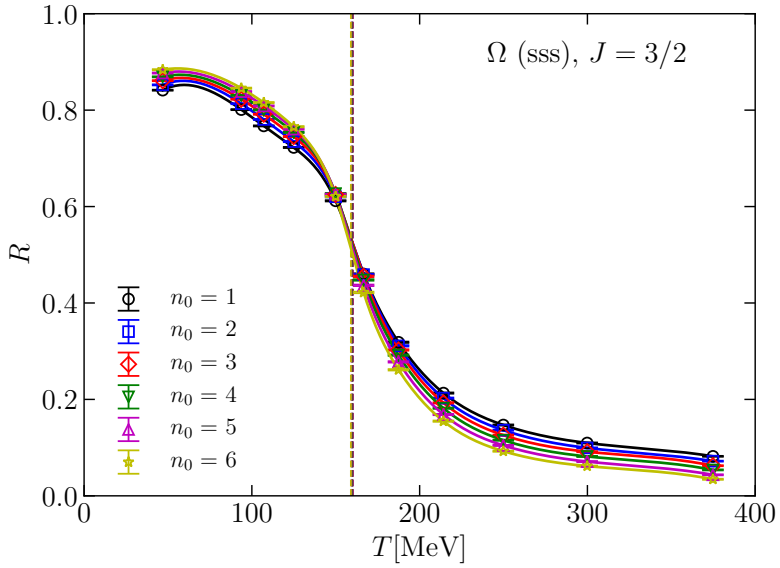

Figure 52: As above, for 32-Omega-sss.

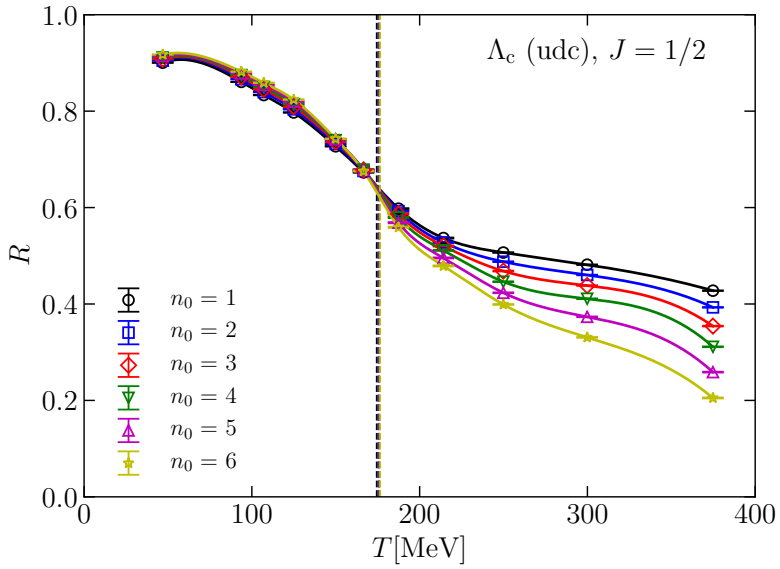

Figure 53: As above, for 12-Lambda_c-udc.

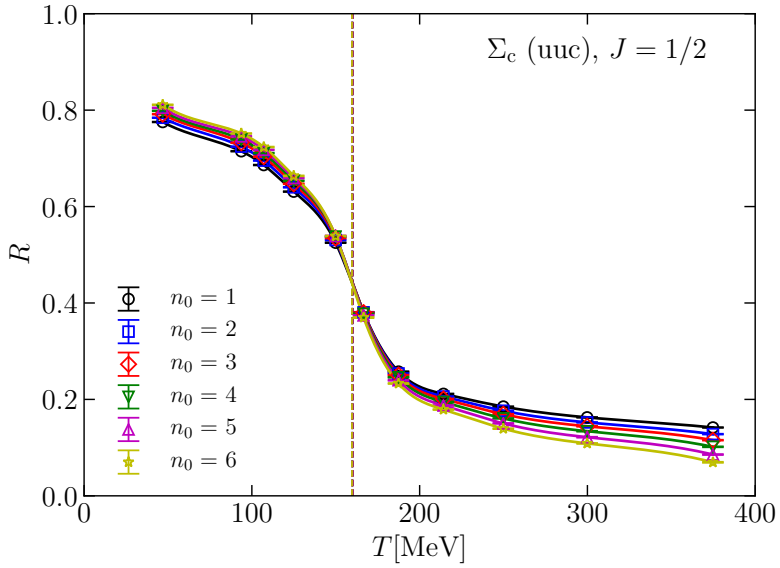

Figure 54: As above, for 12-Sigma_c-uuc.

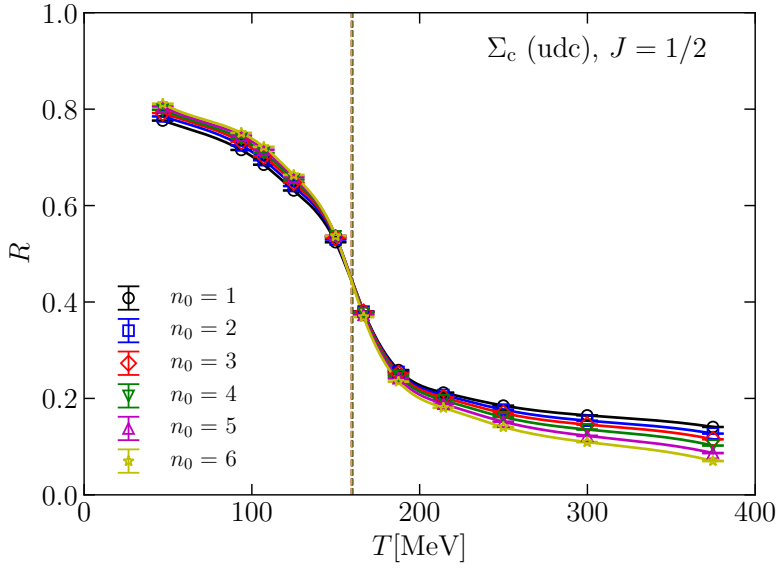

Figure 55: As above, for 12-Sigma_c-udc.

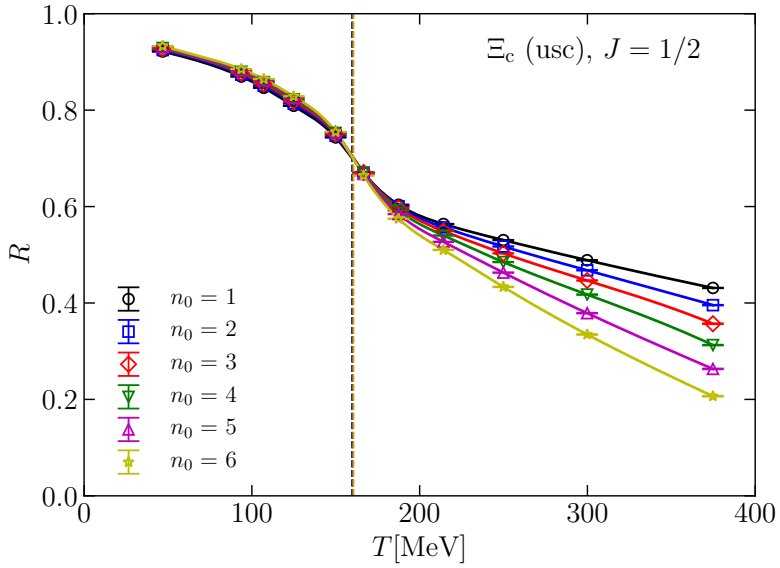

Figure 56: As above, for 12-Xi_c-usc.

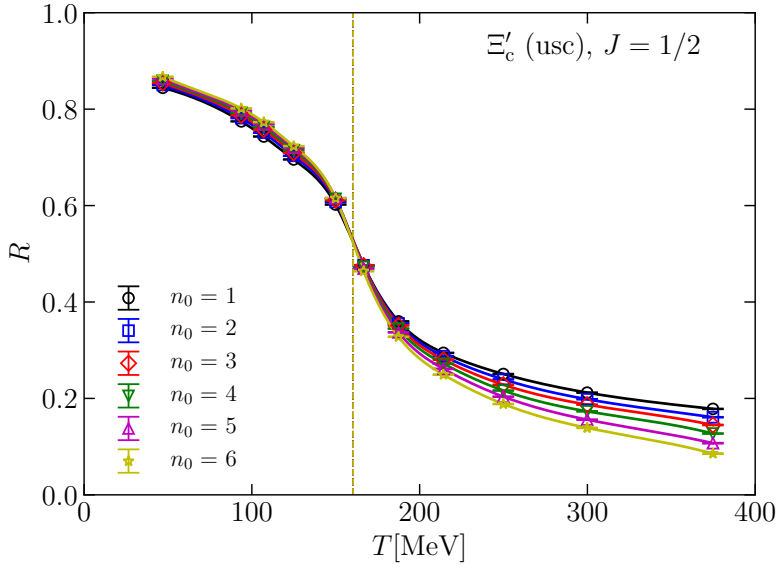

Figure 57: As above, for 12-Xi_c-prime-usc.

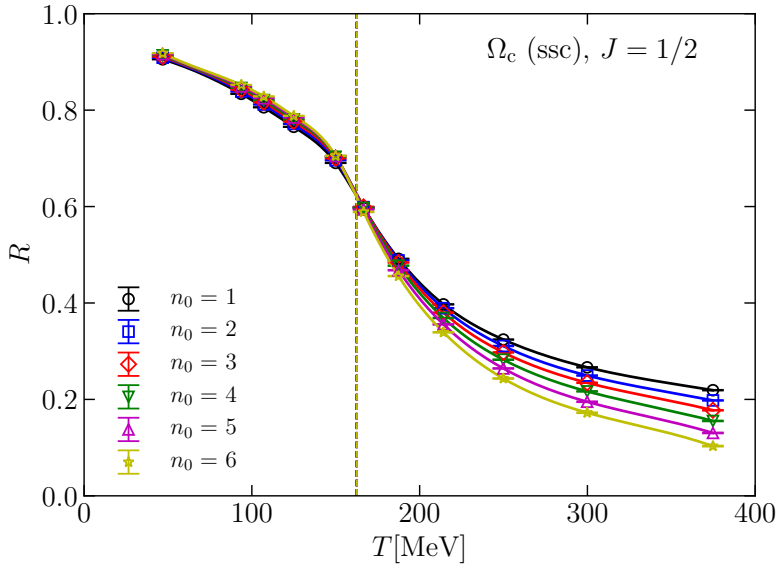

Figure 58: As above, for 12-Omega_c-ssc.

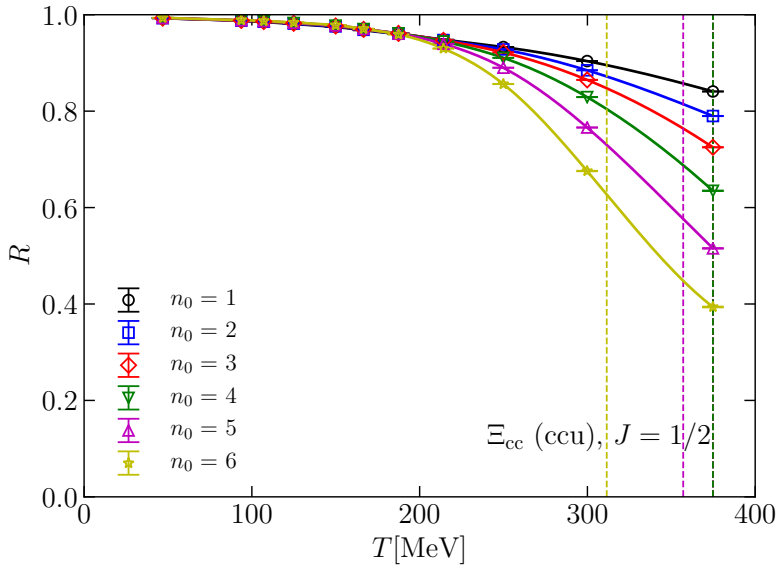

Figure 59: As above, for 12-Xi_cc-ccu.

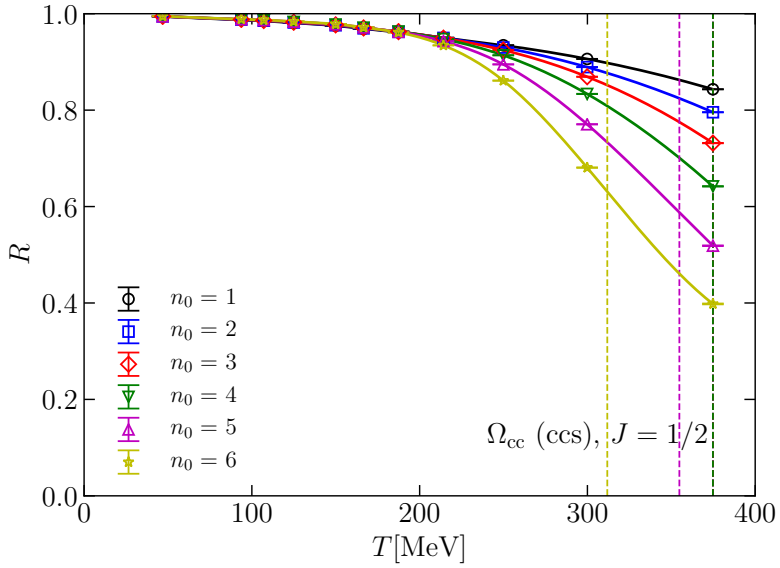

Figure 60: As above, for 12-Omega_cc-ccs.

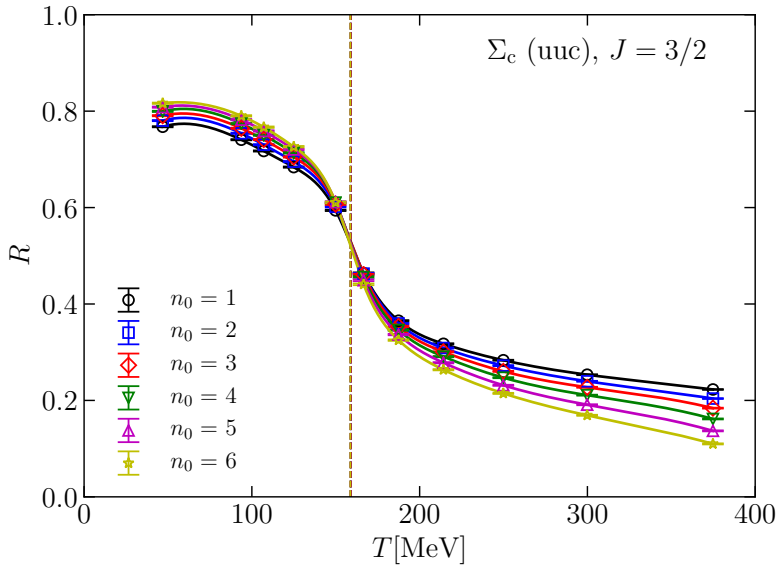

Figure 61: As above, for 32-Sigma_c-uuc.

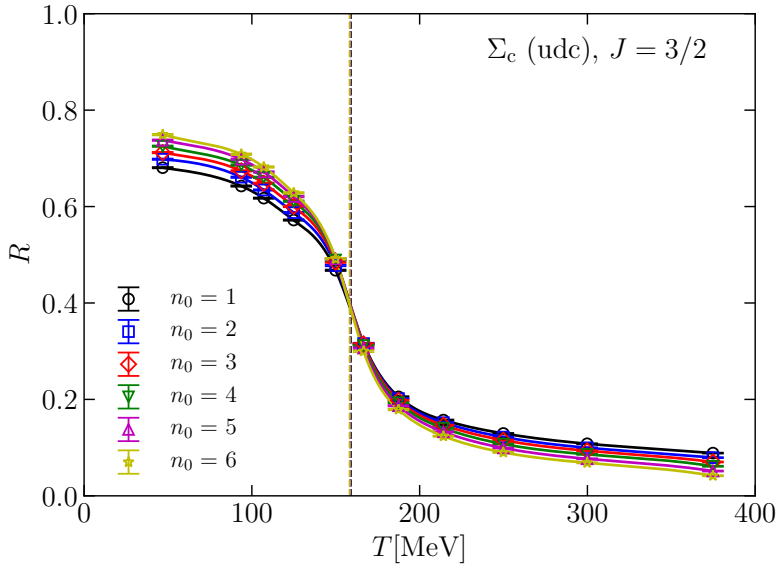

Figure 62: As above, for 32-Sigma_c-udc.

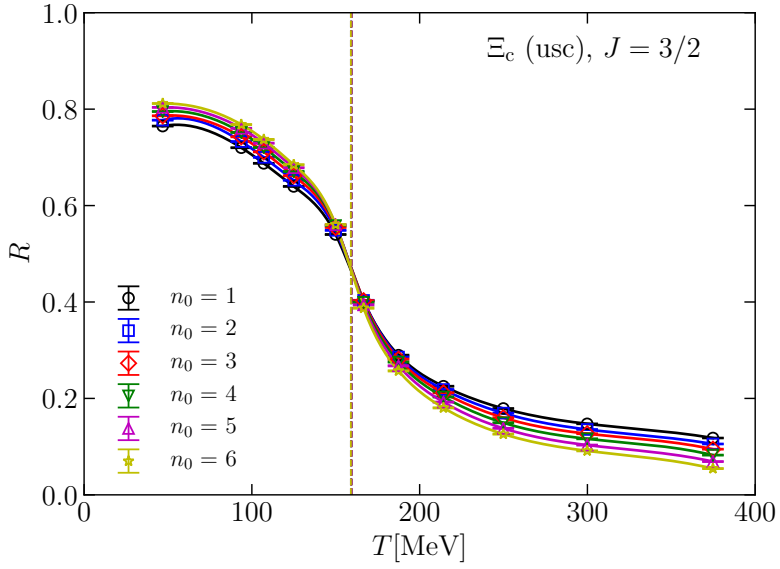

Figure 63: As above, for 32-Xi_c-usc.

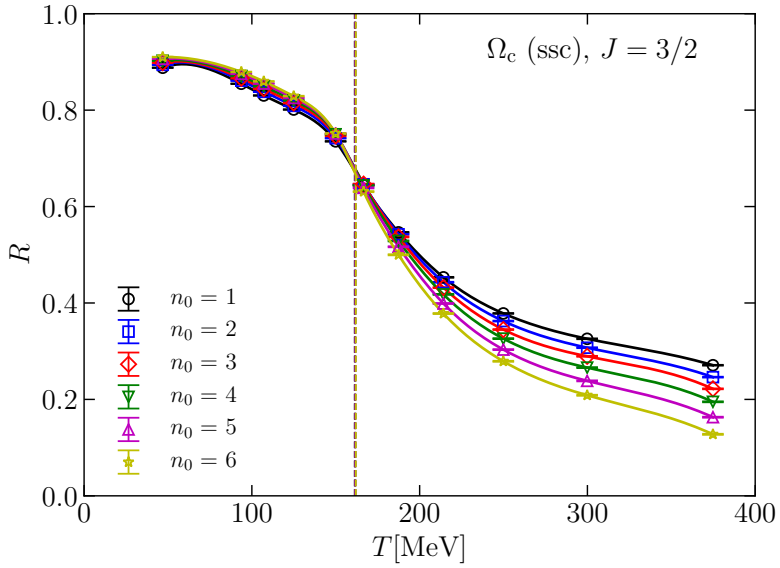

Figure 64: As above, for 32-Omega_c-ssc.

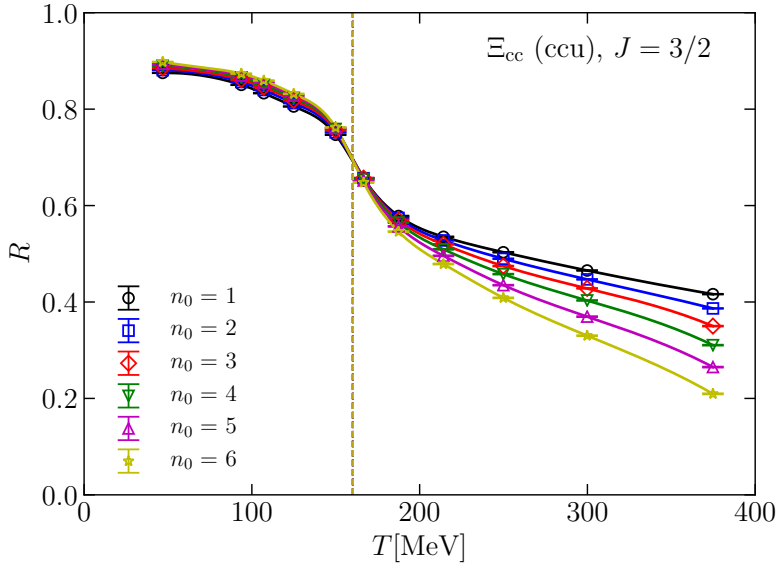

Figure 65: As above, for 32-Xi_cc-ccu.

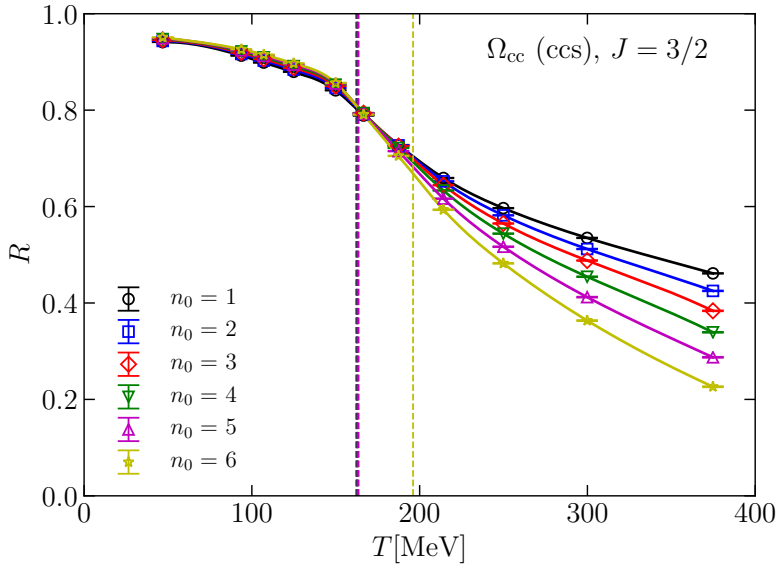

Figure 66: As above, for 32-Omega_cc-ccs.

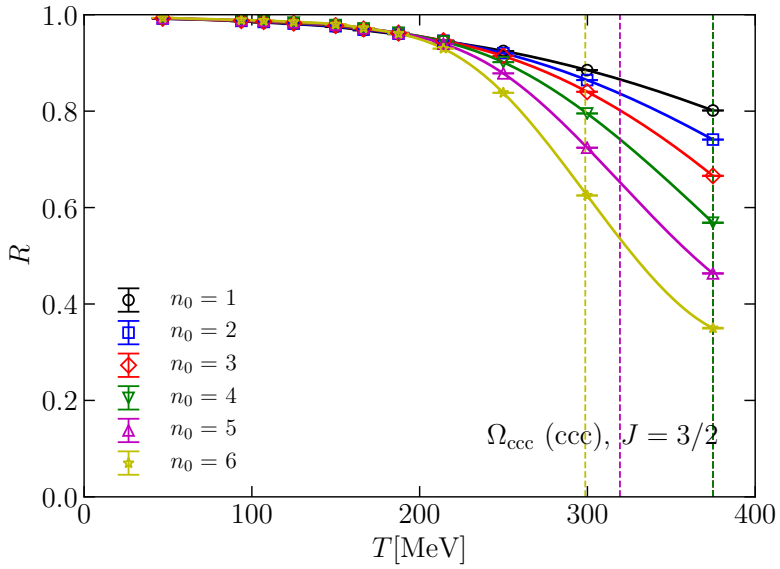

Figure 67: As above, for 32-Omega_ccc-ccc.